

THE mRNA ELEMENTS DIRECTING PREFERENTIAL TRANSLATION IN THE
INTEGRATED STRESS RESPONSE

Parth Hitenbhai Amin

Submitted to the faculty of the University Graduate School

in partial fulfillment of the requirements

for the degree

Doctor of Philosophy

in the Department of Biochemistry and Molecular Biology,

Indiana University

September 2022

Accepted by the Graduate Faculty of Indiana University, in partial fulfillment of the requirements for the degree of Doctor of Philosophy.

Doctoral Committee

Ronald C. Wek, Ph.D., Chair

X. Charlie Dong, Ph.D.

July 15, 2022

Jeffrey S. Elmendorf, Ph.D.

Amber L. Mosley, Ph.D.

© 2022

Parth Hitenbhai Amin

DEDICATION

This dissertation is dedicated to my parents and my aunt Geeta who have loved and supported me throughout this journey.

ACKNOWLEDGEMENTS

Foremost, I would like to thank Dr. Ronald C. Wek for giving me the opportunity to work in his laboratory. I am highly indebted to Dr. Wek for being an exemplary mentor and for his invaluable guidance and support. I would like to individually thank all my thesis committee members: Dr. Amber L. Mosley, Dr. Jeffrey S. Elmendorf, and Dr. X. Charlie Dong for their time and valuable suggestions for my research project. Furthermore, I would like to thank Dr. Jeffrey Allen Willy and Dr. Howard Masuoka for playing a valuable role in my advisory committee meetings. I would like to convey special thanks to Dr. Kirk A. Staschke and Sheree Wek for their constant support and help throughout my graduate education.

I would like to acknowledge members of the Wek lab for technical assistance and helpful discussions. This includes Kenneth R. Carlson for assistance in polysome profiling, Ricardo Cordova for microscopy, Dr. Jagannath Misra and Dr. Michael Holmes for sharing polysome analysis protocols. I would like to thank former Wek lab member Dr. Leonardo Augusto for giving me a chance to be a part of multiple exciting collaborative projects. A special thanks to Dr. Rebecca R. Miles and Riazul Alam for the valuable career advice. I would like to thank former Wek lab Research Associate Erika Dobrota for her help in training when I first joined the Wek lab.

I would like to thank our long-term collaborator Dr. Tracy Anthony for her valuable insights for my research project. I would also like to thank the entire staff of

Biochemistry and Molecular Biology Department and IBMG Graduate Office for their support.

I would like to thank all my friends over here who became a family for their constant support and for creating unforgettable memories in Indianapolis. I would like to specially thank my wife Sunayana for her constant support and understanding throughout this Ph.D. journey. Lastly, I would like to express my deep gratitude to my parents and my aunt Geeta for their endless love, sacrifice, support, and encouragement to achieve my study goals.

Parth Hitenbhai Amin

THE mRNA ELEMENTS DIRECTING PREFERENTIAL TRANSLATION IN THE
INTEGRATED STRESS RESPONSE

In response to environmental and physiological stresses, cells impose translational control to reprogram adaptive gene expression and conserve energy and nutrients. A central mechanism regulating translation involves phosphorylation of the α -subunit of the eukaryotic initiation factor -2 (p-eIF2 α), which reduces delivery of initiator tRNA to ribosomes and represses global protein synthesis. The pathway featuring p-eIF2 α is called the integrated stress response because it involves multiple related eIF2 α kinases, each responding to different stress arrangements. While p-eIF2 α limits global protein synthesis, a subset of mRNAs are preferentially translated in response to p-eIF2 α . Preferential translation of stress adaptive mRNAs is regulated by upstream opening reading frames (uORFs) present in the 5'-leader of these transcripts. In most cases uORFs are inhibitory in nature, but in some case uORFs can instead promote the translation of the downstream CDS. This study is focused on preferential translation of the gene Inhibitor of Bruton's Tyrosine Kinase-alpha (*IBTK α*) in response to endoplasmic reticulum stress. The human *IBTK α* gene encodes a 1353 amino acid residue protein, along with a 5'-leader featuring predicted canonical uORFs. Among the four predicted uORFs, the 5'-proximal uORF1 and uORF2 are phylogenetically conserved among mammals and are well translated as judged by reporter assays, whereas uORF3 and uORF4 are not conserved and are poorly translated. In addition to the uORFs in the *IBTK α* mRNA, a phylogenetically conserved stem-loop (SL) of moderate stability is

present 11 nucleotides downstream of uORF2. Using luciferase reporter assay, the uORF2 and SL were shown to function together to repress the translation of human *IBTK α* . In non-stressed conditions, the SL combined with uORF2 are critical for reducing ribosomes from reinitiating at the *IBTK α* coding sequence (CDS), thus repressing *IBTK α* expression. Upon ER stress and induced p-eIF2 α , the more modestly translated uORF1 facilitates the bypass of the inhibitory uORF2/SL to enhance the translation of main CDS of *IBTK α* . This study demonstrates that uORFs in conjunction with RNA secondary structures can be critical elements that serve as a “bar code” by which scanning ribosomes decide which mRNAs are preferentially translated in the integrated stress response.

Ronald C. Wek, Ph.D., Chair

X. Charlie Dong, Ph.D.

Jeffrey S. Elmendorf, Ph.D.

Amber L. Mosley, Ph.D.

TABLE OF CONTENTS

LIST OF TABLES	xi
LIST OF FIGURES	xii
LIST OF ABBREVIATIONS.....	xiv
CHAPTER 1. INTRODUCTION.....	1
1.1 Gene expression and translation initiation.....	1
1.2 Regulation of translation by mRNA elements	3
1.3 Regulation of translation initiation during the integrated stress response	8
1.4 Diverse cellular stresses activate the ISR	9
1.5 Role of uORFs in regulating translation in ISR.....	14
1.6 Regulation of translation by delayed reinitiation in ISR	15
1.7 Regulating ISR translation by the bypass mechanism.....	18
1.8 Role of RNA secondary structure in regulating translation in ISR	21
1.9 ISR in disease.....	22
1.10 Human <i>IBTKα</i> is preferentially translated in response to ER stress.....	23
CHAPTER 2. EXPERIMENTAL PROCEDURES.....	26
2.1 Cell culture.....	26
2.2 Immunoblot analyses	30
2.3 Plasmid constructions	31
2.4 Luciferase reporter assays.....	38

2.5 Polysome profiling and sucrose gradient ultracentrifugation	39
2.6 RNA isolation and RT-qPCR	40
2.7 Statistical analysis.....	41
CHAPTER 3. RESULTS	42
3.1 Multiple regulatory elements are present in the 5'-leader of human <i>IBTKα</i> mRNA.....	42
3.2 The uORF2 functions as a major inhibitory element in <i>IBTKα</i> translational control	49
3.3 The SL functions in conjunction with uORF2 to regulate <i>IBTKα</i> translation.....	58
3.4 The SL functions in conjunction with uORF2 to thwart translation reinitiation	64
CHAPTER 4. DISCUSSION.....	69
4.1 Translational control of human <i>IBTKα</i>	69
4.2 RNA elements that confer preferential translation in the ISR	73
4.3 RNA structurome in the ISR.....	77
4.4 Significance of this study.....	78
4.5 Implications of <i>IBTKα</i> in the ISR implementation and function.....	79
REFERENCES	81
CURRICULUM VITAE	

LIST OF TABLES

Table 1. List of <i>IBTKα</i> guide sequences and primer sequences.....	28
Table 2. List of different <i>IBTKα</i> -Luc and <i>ATF4</i> -Luc reporters.....	33
Table 3. Raw values of firefly and nano luciferase from HEK293T cells transfected with the WT version of P_{CMV} - <i>IBTKα</i> -Luc reporter and treated with thapsigargin or vehicle.	54

LIST OF FIGURES

Figure 1. Transcriptional and translational control can increase protein levels.	6
Figure 2. Schematic of different elements of mRNA that can contribute to translation control.	7
Figure 3. Schematic of integrated stress response.	13
Figure 4. Regulation of <i>ATF4</i> expression by the delayed translation reinitiation mechanism.	17
Figure 5. Regulation of <i>GADD34</i> expression through delayed translation reinitiation mechanism.	20
Figure 6. Schematic of different domains of human <i>IBTKα</i> protein.	25
Figure 7. Conserved SL of human <i>IBTKα</i> mRNA is important for its translational control.	44
Figure 8. Validation of <i>IBTKα</i> antibody by immunoblot using HEK293 <i>IBTKα</i> KO cells.	46
Figure 9. Human <i>IBTKα</i> mRNA shift towards polysomes during ER stress.	47
Figure 10. <i>IBTKα</i> mRNA is preferentially translated in response to ER stress.	52
Figure 11. Preferential translation of <i>IBTKα</i> during ER stress is dependent on the activity of eIF2 α kinase PERK.	55
Figure 12. Translational control of <i>IBTKα</i> features an inhibitory uORF2.	56
Figure 13. The conserved SL regulates <i>IBTKα</i> translation by functioning in conjunction with inhibitory uORF2.	60
Figure 14. Conserved SL regulates <i>IBTKα</i> translation by contributing to the repressing function of uORF2.	62

Figure 15. Distance between the SL and uORF2 is critical for translational control of *IBTK α* 63

Figure 16. The SL and uORF2 regulates *IBTK α* translation by blocking translation reinitiation. 66

Figure 17. The property of *IBTK α* SL to block reinitiation is transferrable to heterologous system that contains 5' leader of mouse *ATF4*. 68

Figure 18. Model of preferential translation of human *IBTK α* 72

Figure 19. Different functions of uORFs in the ISR..... 75

LIST OF ABBREVIATIONS

AAVS1	Adeno-Associated Virus Site 1
ABC	ATP Binding Cassette
ANK	Ankyrin Repeat
ATF	Activating Transcription Factor
BTB	Broad-Complex, Tramtrack and Bric a brac
C/EBP	CCAAT/Enhancer Binding Protein
CARE	C/EBP-ATF Response Element
CAT1	Cationic Amino Acid Transporter 1
CDS	Coding Sequence
CHOP	C/EBP Homologous Protein
CReP	Constitutive Repressor of eIF2 Phosphorylation
CUL3	Cullin3
DMSO	Dimethyl Sulfoxide
eEF	Eukaryotic Elongation Factor
eIF	Eukaryotic Initiation Factor u
ER	Endoplasmic Reticulum
ERAD	Endoplasmic Reticulum Associated Degradation
eRF	Eukaryotic Release Factor
FRT	Flippase Recognition Target
GADD34	Growth Arrest and DNA Damage-Inducible Protein 34
GCN2	General Control Nonderepressible-2
GEF	Guanine Nucleotide Exchange Factor

HRI	Heme Regulated Inhibitor
IBTK α	α Isoform of Inhibitor of Bruton's Tyrosine Kinase
IBTK β	β Isoform of Inhibitor of Bruton's Tyrosine Kinase
IBTK γ	γ Isoform of Inhibitor of Bruton's Tyrosine Kinase
ICE	Inference of CRISPR Edits
IRE	Iron Responsive Element
IRES	Internal Ribosome Entry Site
IRP	Iron Regulatory Protein
ISR	Integrated Stress Response
KO	Knock-Out
MEHMO	Mental Deficiency, Epilepsy, Hypogonadism, Microcephaly, and Obesity
mRNA	Messenger RNA
p-eIF2 α	Phosphorylation of the α Subunit of Eukaryotic Initiation Factor 2
PABP	Poly (A) Binding Proteins
PCR	Polymerase Chain Reaction
PERK	PKR-like Endoplasmic Reticulum kinase
PIC	Preinitiation Complex
PKR	Protein Kinase RNA
PP1	Protein Phosphatase 1
PVOD	Pulmonary Veno Occlusive Disease
RBP	RNA Binding Protein
RCC1	Regulator of Chromatin Condensation 1
RISC	RNA Induced Silencing Complex

rRNA	Ribosomal RNA
RT-qPCR	Reverse Transcription- Quantitative PCR
SL	Stem-Loop
Tg	Thapsigargin
tRNA	Transfer RNA
uORF	Upstream Open Reading Frame
UTR	Untranslated Region
VWM	Vanishing White Matter
WRS	Wolcott-Rallison syndrome
WT	Wild-Type

CHAPTER 1. INTRODUCTION

1.1 Gene expression and translation initiation

Gene expression is a complex and highly regulated process featuring synthesis and decay of mRNAs and proteins. Much of the focus of gene expression studies is on the measurement of mRNA abundance. However, there is often a poor correlation between mRNA and protein levels (1). This in part is because translation is a major regulator of gene expression. Translation is a process by which new proteins are synthesized via ribosomes using mRNAs as a template. There are four phases of translation: initiation, elongation, termination, and ribosome recycling, with initiation being the most regulated. During the translation initiation phase, a ternary complex consisting of initiator Met-tRNA_i^{Met} and eIF2 coupled to GTP associates with 40S ribosomal subunits and additional initiation factors to form a 43S preinitiation complex (PIC) (2-4). The 43S PIC associates with the 5'-end of mRNAs and scans it in a 5' to 3' direction until it recognizes an appropriate initiation codon. The identification of the initiation codon by the 43S PIC is facilitated through the formation of the base pairs between initiator tRNA and the start codon. Upon base-pair formation, the eIF2 with GTP hydrolyzed to GDP is released from the PIC. This process will situate initiator Met-tRNA_i^{Met} in the P-site of the ribosome, and the 60S ribosomal unit will subsequently join with the 40S ribosomal subunit to form a fully active 80S ribosome (2-4). The elongation process of translation then ensues, with the aid of translation elongation factors. The eukaryotic translation elongation factor 1A (eEF1A) bound to GTP forms a ternary complex with aminoacyl-tRNA, which are brought to the ribosome A site. If the tRNA anticodon sequence matches with the mRNA codon, the aminoacyl-tRNA is retained.

The stability of the base pairing interaction triggers GTP hydrolysis and eEF1A-GDP complex is released and the aminoacyl-tRNA is situated into the A site of ribosome. Formation of peptide bonds via peptidyl transferase activity of ribosomes, results in the transfer of the nascent polypeptide to the peptidyl-tRNA situated in the A site. During the translocation step facilitated by eEF2, the peptidyl-tRNA is moved fully into the P site of the ribosome, while deacylated tRNAs are moved from the P to E site (5,6).

The cycle of elongation steps continue as the ribosome progresses along the mRNA coding sequence. Once the elongating ribosome encounters a stop codon in the A site, the eukaryotic release factors (eRFs) initiate translation termination. During the termination phase, the complex consisting of eRF1-eRF3-GTP binds to the stop codon and GTP hydrolysis releases eRF3 and promotes the cleavage of the ester linkage between the nascent polypeptide and tRNA, facilitating dissociation of the polypeptide from the translation machinery. Though the polypeptide chain is released, the 80S ribosome, deacylated tRNA, and eRF1 are still bound to mRNA. During the ribosome recycling phase (6-8), dissociation of ribosomal subunits is mediated by the multifunctional ATP binding cassette (ABC)-family protein ABC subfamily E member 1 (ABCE1). ABCE1 transforms the chemical energy obtained from ATP hydrolysis for mechanical motion that promotes the dissociation of ribosomal subunits. First, the 60S ribosomal subunit will dissociate from the mRNA, followed by the release of the 40S ribosomal subunit. The ribosomal subunits are then recycled for the next round of translation initiation.

1.2 Regulation of translation by mRNA elements

Translational control is defined as the changes in the efficiency of translation of an mRNA. Translation can be viewed as regulated via global or gene-specific. In global control, translation of most mRNAs is viewed as being controlled in a similar direction. For example, cells respond to stress by diminishing bulk protein synthesis. By comparison, gene-specific regulation focuses on translation of select mRNAs. These translation control schemes involve shared and distinct elements present in eukaryotic mRNAs (9-11). With the changes in translation efficiencies, mRNA levels often do not correlate with amounts of proteins. Illustrating this point, there is transcription induction and translation induction as depicted in Figure 1. In the transcription induction mode, an increase in mRNA abundance can lead to a similar increase in protein synthesis. On the other hand, in translation induction mode there is an increase in protein synthesis without an increase in mRNA abundance (1). A combination of transcription and translation induction schemes of different mRNAs are often observed during stress.

As illustrated in Figure 2, most eukaryotic mRNAs have a 5'-cap and 3'-poly(A) tract and are divided into three regions: the 5'-leader, coding sequence (CDS) for the synthesized polypeptide, and a 3'-untranslated region (UTR). The 5'-cap protects mRNAs from exonuclease-mediated degradation and serves as a docking site for the recruitment of protein complexes involved in RNA processing, export, and translation initiation. The eIF4F protein complex associates with the 5'-cap structure and facilitates the loading of 43S PIC to the mRNA by interacting with the eIF3 protein associated with the 43S PIC (2-4,12). The poly(A) tract on the 3'-end of an mRNA promotes mRNA stability and translation initiation. Poly(A)-binding proteins (PABP) associates with the

poly(A) tract and prevents deadenylation and subsequent mRNA decay. PABP also interacts with the eIF4F complex and is suggested to circularize mRNAs, thus bringing the 3'-UTR in proximity to the 5'-end of the mRNA. Circularization of mRNAs promote translation initiation and ribosome recycling. The shortening of the poly(A) tail reduces association with PABP, thus enhancing mRNA decay and lowering translation (13,14).

Critical elements can be localized in the mRNAs that confer translation regulation (Figure 2). For example, in the 5'-leader region there can be upstream open reading frames (uORFs), RNA stem-loops, and association sites for RNA-binding proteins (15). The uORFs are short ORFs located in the 5'-leader encoding a polypeptide at least 2 amino acid residues in length. uORFs can regulate translation by various mechanisms as described more fully below. Bioinformatic analyses reveal that over half of human transcripts possess at least one predicted uORF in their 5'-leader (16-18). The prevalence of uORFs in human transcripts supports the idea that uORFs have an important function in the regulation of gene expression.

RNA stem-loop structures present in the 5'-leader can regulate translation by structural hinderance which can thwart or pause scanning ribosomes based on position and stability of the RNA structures (11,19). Furthermore, internal ribosome entry sequences (IRES) elements are cis-acting RNA structures that facilitate cap-independent translation by direct recruitment of the 43S PIC complex onto the mRNA (4,11) (Figure 2). The single-stranded, positive-sense picornavirus RNA genomes have well characterized IRES, which serves to recruit the infected host translational machineries independent of eIF4F (20). Certain cellular mRNAs can also have IRES-directed translation. For example, as will be described in more detail in section 1.8 the expression

of *CAT1* CDS is favored by an alteration in the IRES structure in response to stress (21,22).

The 5'-leader can also possess specific motifs which are recognized by RNA binding proteins (RBPs) to regulate translation (Figure 2). In response to iron deficiency in cells, the iron regulatory proteins IRP1 and IRP2 can bind to a stem-loop motif called the iron responsive element (IRE) that is situated in the 5'-leader of ferritin encoding mRNA, blocking the 43S PIC loading onto the 5'-cap of the transcript, thus sharply lowering synthesis of the subunits of this iron storage protein (23,24). The codon composition of the CDS can also affect the rate of translation elongation. The elongation rate can increase with optimal codons, whereas elongation slows down with contiguous rare codons that can cause ribosome pausing and inefficient termination (25).

The 3'-UTR region of an mRNA can also regulate gene expression. There can be binding sites for microRNAs or proteins, along with RNA structures in the 3'-UTRs of mRNA that can confer translation regulation and affect mRNA stability (Figure 2). The binding of microRNAs at complementary sites in the 3'-UTR regions reduces translation by mechanisms suggested to lower translation initiation and enhance RNA induced silencing complex (RISC)-directed mRNA degradation (26). RNA stem-loops situated in the 3'-UTR can also function as a docking site for RNA binding proteins that can regulate mRNA translation via mechanisms involving the proximity of the 5'- and 3'-ends of mRNA in closed loops (27).

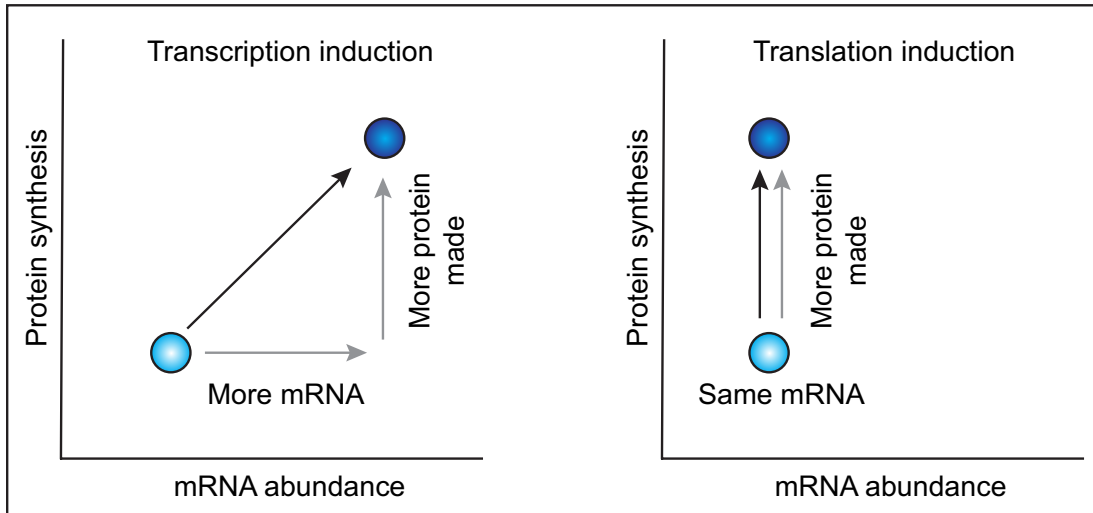


Figure 1. Transcriptional and translational control can increase protein levels.

In transcriptional regulation, increased amounts of mRNA that are efficiently translated lead to proportionally more protein. In translational control, amounts of mRNA do not change, but there is enhanced efficiency of translation, leading to more synthesized protein.

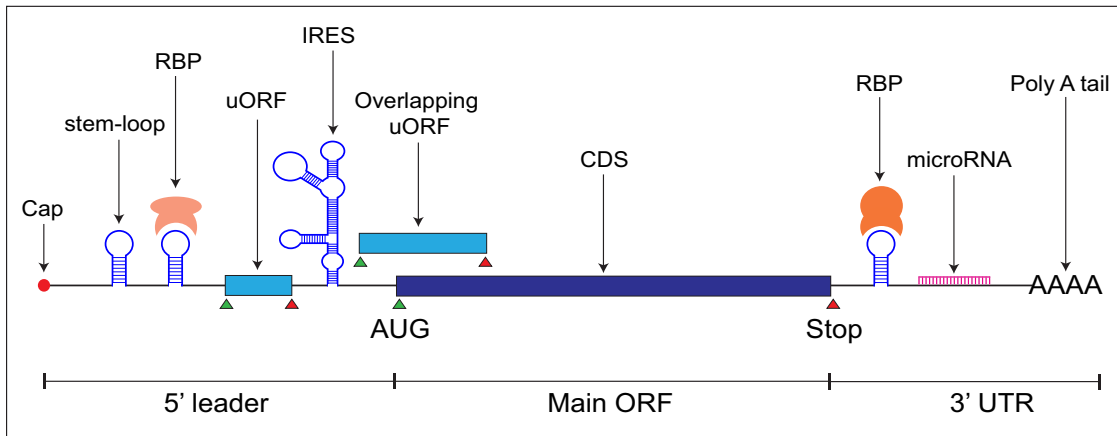


Figure 2. Schematic of different elements of mRNA that can contribute to translation control.

The mRNA is depicted with the 5'-cap and 3'-polyadenylation tract. Non-overlapping and overlapping uORFs situated in the 5'-leader are presented as light blue boxes, with the CDS presented as purple box. In the CDS, a green triangle represents the start codon, and a red triangle represents the stop codon. RNA stem loops can be present in 5'-leader and 3'-UTR. Certain RNA structures can be recognized by RNA binding proteins (RBP). IRES are situated in the 5'-leader of certain cellular and viral mRNAs, facilitating direct loading of the PIC for cap-independent translation. Binding sites for microRNAs can be situated at the 3'-UTR of mRNAs, facilitating translation repression and mRNA decay via the RISC.

1.3 Regulation of translation initiation during the integrated stress response

In response to various physiological and environmental stresses, cells invoke translational control to reprogram gene expression directed towards conserving energy and nutrients. A central mechanism governing the regulation of translation during stress involves phosphorylation of the α subunit at Serine 51 of the translation initiation factor-2 (eIF2). The pathway featuring phosphorylation of eIF2 α (p-eIF2 α) is called the integrated stress response (ISR) as it involves multiple eIF2 α kinases, each responding to different stress conditions. Increased p-eIF2 α during stress blocks global translation, with most mRNAs being repressed. On the other hand, p-eIF2 α can also facilitate preferential translation of a certain subset of mRNAs that are stress adaptive (9,10,28). As described earlier in section 1.1, the eIF2 couples with GTP and serves to deliver initiator tRNA in the PIC. During the process by which initiator tRNA recognizes the initiation codon in the ribosome P site, the GTP associated with eIF2 is hydrolyzed to GDP and eIF2-GDP is released from the 40S ribosome bound to the mRNA (2,4). For the next round of translation initiation, the GDP bound to eIF2 must be exchanged to GTP via a guanine nucleotide exchange factor (GEF) eIF2B.

The eIF2B is a heterodecamer, composed of a dimer of a pentamers of five different subunits designated α , β , δ , γ and ϵ . The GTP binding site resides in eIF2B γ and the nucleotide exchange catalytic site reside in eIF2B ϵ . During stress, p-eIF2 α binds to eIF2B and allosterically switches eIF2B from its active state to an inhibited state, thus preventing the engagement of eIF2-GDP to eIF2B and inhibiting the GDP to GTP nucleotide exchange on eIF2. In this way, p-eIF2 α serves as an inhibitor of eIF2B and

decreases the levels of eIF2/GTP/Met-tRNA_i^{Met} in the cells (29,30). As a consequence, induced p-eIF2 α sharply reduces the initiation phase of translation in stressed cells.

Dephosphorylation of p-eIF2 α is carried out by the serine/threonine protein phosphatase 1 (PP1). PP1 dephosphorylation of p-eIF2 α requires specific targeting subunits, including CReP (PPP1R15b), which is generally viewed as being constitutively expressed (31), and GADD34 (PPP1R15a), whose expression is induced by transcriptional and translational mechanisms during the ISR and thus functions in the feedback resumption of translation (32-34). In this way, the levels of p-eIF2 α are controlled by a combination of the activities of eIF2 α kinases and PP1-associated with targeting subunits. Furthermore, induction of GADD34 helps to ensure that the levels of p-eIF2 α and the translational control are self-limiting in the ISR during acute stress.

1.4 Diverse cellular stresses activate the ISR

In mammals, four different protein kinases catalyze p-eIF2 α in response to different stress arrangement. These eIF2 α kinases include heme-regulated inhibitor kinase (HRI; EIF2AK1), protein kinase RNA (PKR; EIF2AK2), PKR-like endoplasmic reticulum kinase (PERK; EIF2AK3), and general control nonderepressible-2 (GCN2; EIF2AK4) (Figure 3). Each of these eIF2 α kinases possess distinct regulatory domains juxtaposed to a shared kinase catalytic region, which allows each to sense a different combination of stress conditions (9,35). For example, heme deprivation, oxidative stress, mitochondrial stress, and heat shock induces HRI phosphorylation of eIF2 α (36,37). PKR participates in an interferon-mediated anti-viral response and is activated by the presence of double-stranded RNA that is produced during the course of replication of many viruses

(38,39). Accumulation of unfolded proteins in the endoplasmic reticulum and hypoxia activates PERK (40-42) and GCN2 is induced by amino acid starvation, which leads to accumulation of uncharged tRNAs that is reported to directly bind to a GCN2 regulatory domain homologous to aminoacyl tRNA synthetases (43,44). Furthermore, GCN2 is suggested to be activated by ribosome collisions (45) and UV irradiation (46) (Figure 3).

In addition to these environmental or extrinsic stresses, intrinsic stresses in cells can induce p-eIF2 α . For example, processes associated with cellular differentiation can activate ISR in the certain cell types. Illustrating this idea, during differentiation of keratinocytes, GCN2 and translational control are suggested to help reprogram gene expression and facilitate induction of the differentiated cell morphology (47).

Furthermore, activation of PERK and GCN2 has been reported to be important for differentiation of primed CD4⁺ T cells into cytokine secreting effector cells (48). In cancer cells, gene changes that alter metabolism to enhance growth can activate GCN2 and/or PERK (49). The higher rate of proliferation in cancer cells and altered metabolic demands is suggested to be an intrinsic stress that required uptake of more nutrients and growth factors. Therefore, the ISR helps cancer cells to adapt to their altered metabolic state and promote cancer cell proliferation and survival in certain tumor microenvironments (49).

As described in section 1.3, the ISR features preferential translation of stress adaptive mRNAs. Some of these ISR-target genes encode basic zipper (bZIP) transcription factors, including ATF4, ATF5, and CHOP (50-53). Therefore, the ISR confers regulation of both translation and transcription that together optimizes gene expression strategies to resolve stress. Preferential translation of *ATF4* is a central feature

of the ISR (Figure 3). ATF4 forms heterodimers with other bZIP transcription factors such as C/EBP α , C/EBP β , C/EBP γ and CHOP that can bind to C/EBP-ATF response elements (CARE) in the promoter of ISR target genes (54,55). Preferential translation of *ATF4* upon induced p-eIF2 α enhances the levels of this transcription factor, which directly induces the transcriptional expression of genes involved in amino acid import and synthesis, autophagy, protein synthesis and folding (56,57). Furthermore, ATF4 drives the expression of genes involved in import and metabolism of sulfur-containing amino acids which serve as a precursor of glutathione biosynthesis. Thus, ATF4 target genes confer protection against oxidative stress by maintaining the levels of glutathione in the cells which is a major reductant of endogenous peroxides (56,57). ATF4 also induces the expression of *GADD34*, which plays an important role in feedback regulation of the ISR (32,33). Together, this collection of targeted genes highlights the central role that ATF4 plays in the ISR gene expression to alleviate stress damage.

The process of translation is expensive in the terms of energy consumption, with estimates upwards of 30% of cell ATP consumption, not including that required for synthesis of rRNA and ribosome assembly (58). Furthermore, translation consumes amino acid pools. A critical response of stressed cells is to repress global translation due to p-eIF2 α , to better manage consumption of energy and nutrients, with strategy of stress alleviation. Energy saved instead is redirected to translate stress-related mRNAs and assist folding of damaged proteins as cells strive to restore protein homeostasis. Some of the stress adaptive proteins that are upregulated are molecular chaperones, which are critical for protein folding, and amino acid transporters that serve to enhance uptake of key nutrients (56,59). Protein degradation pathways, such as autophagy and proteasomal

system, are activated to degrade unfolded proteins or protein aggregates and damaged organelles created during stress (60). The recycling of amino acids is also critical for maintaining amino acid levels that drive new protein synthesis.

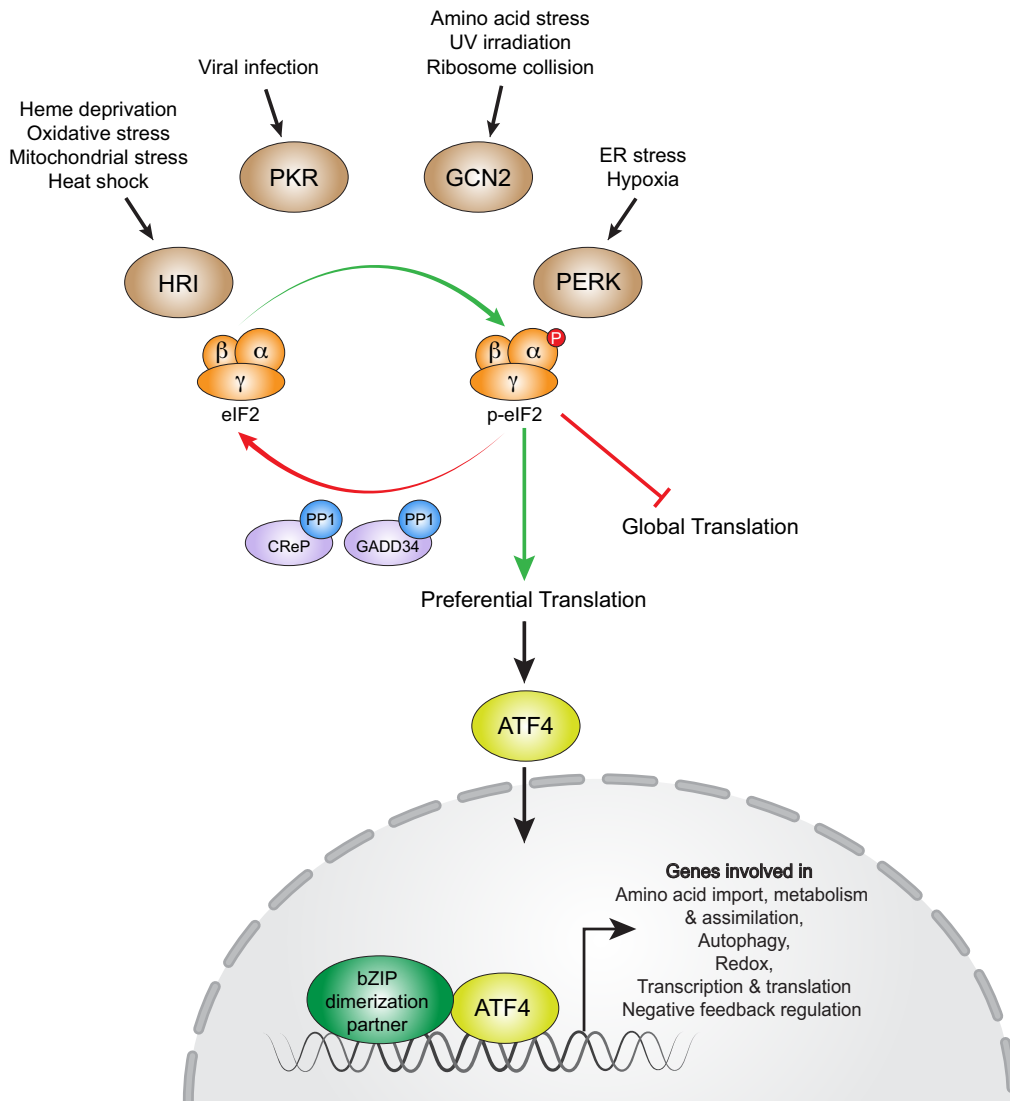


Figure 3. Schematic of integrated stress response.

In response to different stresses, four different mammalian protein kinases catalyze the phosphorylation of α subunit of eIF2. The p-eIF2 α reduces global translation coincident with preferential translation of stress genes like *ATF4*. ATF4 protein translocates to the nucleus and forms a heterodimer with other dimerization partners to induce the expression of downstream targets that function to alleviate the stress. The dephosphorylation of p-eIF2 α is carried out by PP1 partnered with GADD34 or CReP.

1.5 Role of uORFs in regulating translation in ISR

As described earlier in section 1.2, uORFs are *cis*-acting short elements that are critical for differential translation of mRNAs during the ISR. About half of the human transcripts at least possess one predicted uORF with a canonical start codon AUG (16-18). Recent studies based on ribosome profiling also reveal that some transcripts also possess uORFs with non-canonical start codons such as CUG, GUG, and UUG (61,62). The prevalence of uORFs in human transcripts emphasize their significance in regulating gene expression.

In most cases, uORFs are inhibitory and can thwart translation reinitiation at downstream coding sequences. There are many reasons for why an uORF can be inhibitory. For example, the length of an uORF is one determinant for translation reinitiation. Elongating ribosomes are thought to spend more time translating longer uORFs, which reduces the likelihood for retaining critical initiation factors that would aid reinitiation at downstream coding sequences. Retention of critical initiation factors is thought to be more likely when ribosomes translate short uORFs (10,11,63).

Additional processes contributing to inhibitory uORFs involve certain uORF sequences that elicit a pause or stall of elongating ribosomes. In this case, ribosomes require an extended period to elongate and terminate, which is suggested to impede the efficiency of reinitiation. Ribosome pausing during elongation or termination phases is also suggested to cause formation of a ribosome queue along the 5'-leader. Due to ribosome queuing, scanning ribosomes can spend an extended period on start codons of poor context or non-canonical start codon, which enhances the likelihood of initiator tRNA recognition. An uORF can also overlap out-of-frame with a CDS; thus, the

termination codon of uORF is positioned downstream of the main CDS start codon. As a consequence, translation of the overlapping uORF terminates downstream of the main CDS start codon and blocks the ability of the ribosome to recognize the start codon of the CDS. In other cases, uORF can be bypassed in the constitutive fashion or upon induction of stress (10,11,63). Overall, uORFs of diverse properties can be incorporated singly or in combination within mRNAs and as detailed further below can direct specific mechanisms of translation regulation for a given gene.

1.6 Regulation of translation by delayed reinitiation in ISR

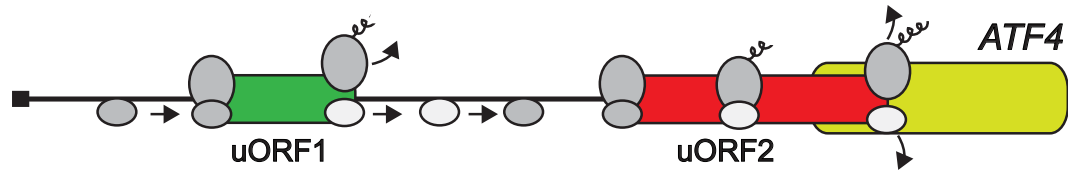
Ribosome reinitiation is one of the predominant mechanisms by which two or more uORFs regulate the translation of downstream CDS and is central to *ATF4* translational control in the ISR. As illustrated in Figure 4, the 5'-leader of mammalian *ATF4* mRNA is about 600 nucleotides in length and encodes two uORFs that have sharply different functions in the preferential translation of *ATF4*. The 5'-proximal uORF1 is only 12 nucleotides long and encodes a 3 amino acid residue polypeptide and is thought to allow for efficient reinitiation at downstream coding sequences. By comparison, uORF2 is 180 nucleotides long and encodes a 59 amino acid residue polypeptide that overlaps out-of-frame with the main *ATF4* CDS. As a consequence, ribosomes translating uORF2 are not able to recognize the CDS initiation codon and instead dissociate from the *ATF4* mRNA; thus, uORF2 is a potent repressor of *ATF4* translation (10,53,57).

During non-stressed conditions, ribosomes adjoined with the eIF2 ternary complex associate with the 5'-end of the *ATF4* mRNA and initiate translation at the 5'-

proximal uORF1. After translation of uORF1, the 40S ribosome resumes scanning and rapidly reacquires eIF2/GTP/Met-tRNA_i^{Met} to reinitiate translation at the next coding sequence- uORF2. As described earlier, the stop codon of uORF2 is present after the initiation codon of *ATF4* CDS. Therefore, following the translation of uORF2 the ribosome dissociates from *ATF4* mRNA, thereby reducing the translation of *ATF4* CDS. During cellular stress, the level of p-eIF2 α is elevated and the availability of eIF2/GTP/Met tRNA_i^{Met} is limited. Therefore, after translating uORF1, the 40S ribosome resumes scanning but it is thought to take a longer to reacquire the limiting eIF2 ternary complex that is required to recognize the next initiation codon. Because of the delay in reacquiring the eIF2 ternary complex, the 40S ribosome scans through inhibitory uORF2 and instead reinitiates at next initiation codon for the *ATF4* CDS. This delayed reinitiation results in preferential translation of *ATF4* CDS (10,53). As highlighted in section 1.4, increased ATF4 protein induces the transcription of genes involved in amino acid transport and amino acid biosynthesis, oxidative stress response genes, and cholesterol metabolism genes (56). The expression of mammalian *ATF5* is also regulated by the delayed reinitiation mechanism by two uORFs (52).

Delayed translation reinitiation

No Stress: High eIF2-GTP, low eIF2 α -P



High Stress: Low eIF2-GTP, high eIF2 α -P

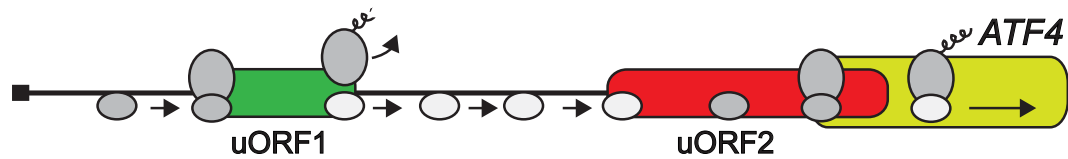


Figure 4. Regulation of *ATF4* expression by the delayed translation reinitiation mechanism.

The uORF1 and 2 in the *ATF4* mRNA are represented as boxes situated upstream of the CDS that encodes the ATF4 protein. A model of translation control of *ATF4* mRNA during stress in the ISR is described in the text. The 40S ribosome with and without eIF2 ternary complex are depicted as dark grey oval and light grey oval respectively. During the translation initiation process, the 40S joins the 60S ribosome, leading to translation elongation and synthesis of nascent polypeptide.

1.7 Regulating ISR translation by the bypass mechanism

The sequence context surrounding the start codon termed the Kozak context is an important determinant for the translation initiation. In vertebrates, the optimal Kozak sequence is GCCA/GCCATGG, with the underlined gene start codon. The positioning of purine at -3 and G at +4 are important as those residues have been shown to interact with eIF2 and 18S rRNA present in the 40S ribosomal subunit. This interaction is thought to promote robust translation initiation from the start codon (64-66). The start codon with non-optimal Kozak or poor Kozak context triggers less efficient translation initiation. In this way, the scanning 43S PIC will initiate translation of an uORF with an optimal Kozak whereas it will bypass the uORF with a poor Kozak context. Therefore, the Kozak context of a uORF plays a significant role in the regulation of translation.

Expression of mammalian *GADD34* is regulated by ribosome bypass of an uORF in the ISR. The 5'-leader of mammalian *GADD34* encodes two uORFs (Figure 5). Both uORF1 and uORF2 have poor Kozak context. uORF1 is not efficiently translated and appears to be a modest dampening element independent of stress conditions. However, the downstream uORF2 can be well translated. In the absence of stress and low p-eIF2 α levels, uORF2 of *GADD34* serves as a major inhibitory uORF for *GADD34* expression. The last three codons before the stop codon of the *GADD34* uORF2 encode for Pro-Pro-Gly-Stop (PPG*). Translation of the PPG* codons of uORF2 is thought to lead to inefficient termination that reduces the efficiency of ribosome reinitiation at downstream *GADD34* CDS. Therefore, there is minimal translation of the *GADD34* during non-stressed conditions. However, upon stress and induced p-eIF2 α , a portion of the scanning ribosomes bypass uORF2 due in part to the poor Kozak context and instead initiates

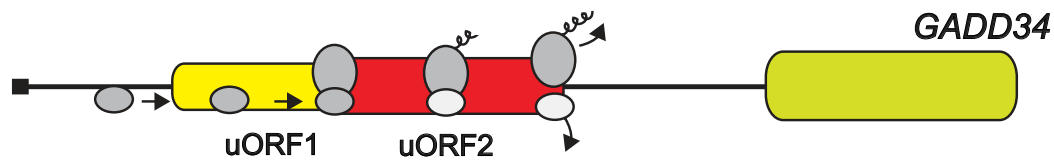
translation at the downstream *GADD34* CDS, thus leading to an increase in GADD34 protein (10,67). As highlighted earlier in section 1.4, transcription of *GADD34* is also enhanced in the ISR during stress; the combination of increased transcriptional and translational expression ensures that there is enhanced GADD34 that contributes to feedback control of the ISR.

Expression of mammalian *CHOP* in ISR is also regulated by mechanism of ribosome bypass via a single uORF. However, in this case the inhibitory uORF thwarts translation reinitiation at the downstream *CHOP* CDS by the stalling of ribosomes translating the uORF (10,50). During stress and increased p-eIF2 α , a subset of ribosomes are thought to proceed through the inhibitory uORF and instead translate the *CHOP* CDS. While the mechanistic features are not well understood, the uORF has a poor start codon context, whereas the CDS is optimal. It is thought that the lowered eIF2 ternary complex during p-eIF2 α can change the flux of scanning ribosomes and possibly the efficiency of start codon recognition, which would allow for a percentage to bypass the inhibitory uORF and instead enhance translation of the *CHOP* CDS during the ISR (10,50,68).

In contrast to an uORF blocking translation reinitiation, a uORF can also promote reinitiation as observed in expression of mammalian *CREP*, which constitutively directs PP1 dephosphorylation of p-eIF2 α . Like *GADD34*, the *CREP* mRNA has two uORFs, with uORF1 only modestly translated and uORF2 translated more efficiently (10,67). However, the uORF2 allows for efficient ribosome reinitiation at the downstream *CREP* CDS. In this way, *CREP* is well translated independent of p-eIF2 α . (10,67).

Start codon dependent ribosome bypass

No Stress: High eIF2-GTP, low eIF2 α -P



High Stress: Low eIF2-GTP, high eIF2 α -P

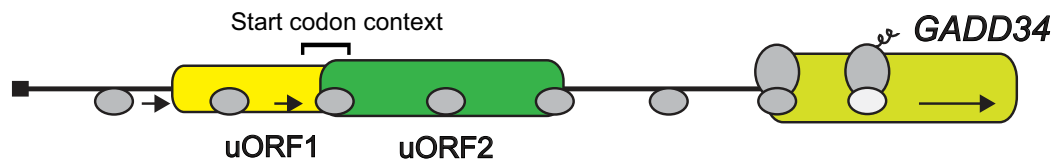


Figure 5. Regulation of *GADD34* expression through delayed translation reinitiation mechanism.

GADD34 uORFs are represented as boxes situated upstream of the CDS encoding the *GADD34* protein. A model of translation control of *GADD34* mRNA during stress in the ISR is described in the text. The 40S ribosome with ternary complex is depicted as dark grey oval and without ternary complex is depicted as light grey oval.

1.8 Role of RNA secondary structure in regulating translation in ISR

RNA secondary structures in the 5'-leader region of an mRNA can serve as key elements that affect the efficiency of translation initiation. The positioning as well as the stability of RNA stem-loops are important determinants in deciding the fate of translation. As detailed for ferritin mRNA in section 1.2, placement of an RNA stem-loop with intermediate or strong stability close to the 5' cap of an mRNA can cause steric hindrance that prevents engagement of the 43S PIC with the mRNA, therefore sharply reducing translation. Inclusion of an RNA stem-loop with strong stability further downstream in the 5'-leader can affect the efficiency of ribosome scanning and the process of initiation. However, RNA structures of intermediate stability can have minimal effect on scanning ribosomes. In fact, placement of an RNA stem-loop with intermediate stability just downstream of an initiation codon is suggested to enhance ribosome recognition of a start codon with poor or suboptimal Kozak context. The secondary RNA structure is thought to slow down or pause a scanning ribosome which gives more time for the 43S PIC to recognize the suboptimal initiation codon (11,19,69). In this way, certain mRNAs are suggested to possess RNA stem-loops to regulate selection of the initiation sites of the CDS. Furthermore, as described in section 1.2, certain cellular mRNAs can also possess RNA secondary structures embedded in the 5'-leader that can function as an IRES. An IRES element can promote the direct loading of 43S PIC complex to the mRNA thereby facilitating cap-independent translation. For example, the cationic amino acid transporter *CATI* mRNA was suggested to have IRES with an embedded uORF (21,22). During the stress conditions, it is suggested that translation of the uORF and elongation pause alters the IRES structure to favor the

translation of *CATI* CDS (21,22). Therefore, an uORF flanking RNA structure in *CATI* can enhance translation via internal ribosome loading mechanisms.

1.9 ISR in disease

The role of ISR in the pathogenesis of various diseases is complex. While the ISR can have important protective functions that ensure health, chronic induction of the ISR can alter this pathway to contribute to disease. Loss of function mutations in PERK and GCN2 impairs the induction of ISR and causes Wolcott-Rallison syndrome (WRS) and pulmonary veno-occlusive disease (PVOD) respectively (70,71). WRS is characterized by early onset diabetes and multiple epiphyseal dysplasia (72,73). PVOD is characterized by pulmonary hypertension arising due to narrowing of pulmonary veins and venules by fibrous tissue (71). In contrast to WRS and PVOD that impair induction of the ISR, there are some diseases that are caused due to the constitutive activation of ISR. The loss of CReP destabilizes the CReP-PP1 complex, thereby increasing p-eIF2 α , leading to patients with intellectual disability, short stature, and diabetes (74,75). Furthermore, mutation in each of the five subunits of eIF2B can cause vanishing white matter (VWM) disease. The eIF2B mutations reduce the activity of eIF2B, which in turn lowers the availability of the eIF2 ternary complex and is suggested to activate the ISR even when p-eIF2 α is low. During stress, basal activation of the ISR combined with further induction of p-eIF2 α leads to a ISR activation that is both higher in magnitude and duration. This inappropriate superinduction of the ISR during stress triggers the loss of myelin and progressive neurological symptoms such as ataxia, spasticity, and cognitive deterioration, the characteristics of VWM (76,77).

MEHMO (mental deficiency, epilepsy, hypogenitalism, microcephaly, and obesity) syndrome is also caused by the reduction in eIF2 ternary complex due to a mutation in gene encoding eIF2 γ , a subunit of the eIF2 complex that is required for GTP binding (78-80). Akin to the description of VWM, the lowered eIF2 activity triggers basal activation of the ISR and leads to a higher and misregulated ISR. Finally, in many types of cancers, activation of ISR promotes tumor initiation and progression. For example, PERK pathway is reported to be activated in prostate cancer and inhibition of PERK has been shown to be beneficial to reduce progression of certain cancer (81).

As highlighted above, disease can stem from hypo or hyper- induction of the ISR. For diseases involving hyper- induction of the ISR, treatment regimens involving small molecule inhibitors of eIF2 α kinases or a small molecule activator of eIF2B may be beneficial (82-85). In contrast those diseases suggested to involve hypo-induction of the ISR, small molecule inhibitors of GADD34-PP1 complex that leads to enhanced p-eIF2 α may confer protection (86-89).

1.10 Human *IBTK* α is preferentially translated in response to ER stress

This thesis addresses the preferential translation of the ISR target gene called Inhibitor of Bruton's Tyrosine Kinase-alpha (*IBTK* α). The human gene *IBTK* is located at the chromosome 6q14.1. The human *IBTK* gene encodes three different isoforms- *IBTK* α (α), *IBTK* β (β) and *IBTK* γ (γ) that are formed due to an alternative transcription start site and an alternative polyadenylation signal. The longer variants of the *IBTK* gene, *IBTK* α possesses 29 exons and encodes a 1353 amino acid residue polypeptide and *IBTK* β possesses 24 exons and encodes a polypeptide 1196 residues in

length. The shortest version is IBTK γ that encodes a 240 amino acid residue polypeptide derived from 5 exons and is highly expressed in human lymphoid cells (90). This thesis is focused on human IBTK α which is the longest isoform and ubiquitously expressed. The structure of IBTK α protein is unknown but based on the amino acid sequence homology, three different domains are predicted: Regulator of chromosome condensation 1 (RCC1) domains, Ankyrin repeats (ANK), and Broad-Complex, Tramtrack and Bric a brac (BTB) domains (Figure 6). Based on related BTB-containing proteins (91,92), this domain of IBTK α is suggested to bind to cullin 3 (CUL3), an E3 ubiquitin ligase that can promote targeted protein degradation (93-95). Previous studies indicate that IBTK α is localized at the endoplasmic reticulum (ER) membrane and ER exit sites. IBTK α was reported to have a role in the induction of autophagy in hepatocytes upon exposure to saturated free fatty acids such as palmitate (93). IBTK α was also previously identified in a high-throughput screen for mouse gene transcripts that are preferentially translated in response to ER stress (28). The 5'-leader of mammalian *IBTK α* mRNA is about 550 nucleotides long and features four predicted uORFs. It is suggested that one or more of these uORFs may serve as inhibitory elements in translation. My thesis research indicates that a critical feature of preferential translation of *IBTK α* involves bypass of an inhibitory uORF2; translation of uORF2 thwarts downstream reinitiation at the *IBTK α* CDS through a phylogenetically conserved RNA secondary structure that is situated just downstream of the uORF2. This study concludes that RNA secondary structures can function in conjunction with uORFs to serve as critical elements of the bar code by which scanning ribosomes delineate preferential translation of gene transcripts in the ISR.

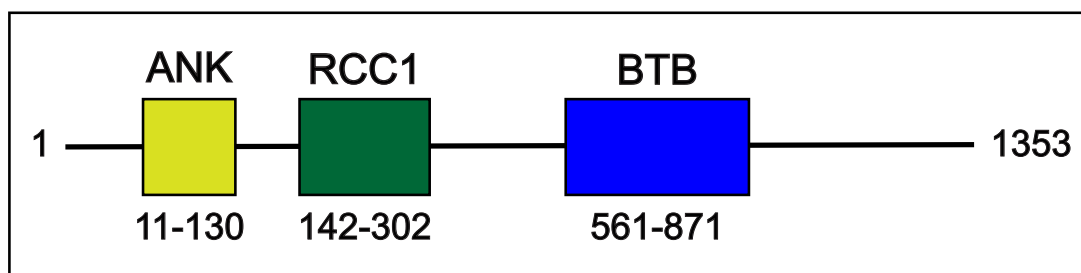


Figure 6. Schematic of different domains of human IBTK α protein.

Three different domains-ANK, RCC1 and BTB are predicted in IBTK α using a sequence homology program InterPro (96,97), These domains are depicted as colored boxes, along with their residue positions in IBTK α . The length of IBTK α is 1353 residues.

CHAPTER 2. EXPERIMENTAL PROCEDURES

2.1 Cell culture

Wild type human embryonic kidney cells with SV40 T antigen (designated HEK293T in this study) were purchased from ATCC (Cat No CRL-3216). Cells were grown in Dulbecco's Modified Eagle Medium (DMEM) media (Corning, Cat No 10-013-CV) supplemented with 10% (v/v) fetal bovine serum (Corning, Cat No 35-010-CV) and 100units/mL penicillin and 100 μ g/ml streptomycin (Cytiva, Cat No SV30010). Human IBTK α KO (knock-out) and IBTK α Δ SL (SL deleted) were derived from HEK293 cells and were obtained from Synthego along with mock transfected WT HEK293 control cells. The RNP-based approach was used to create an indel in exon 2 of the *IBTK α* gene, resulting in a frameshift in the coding sequence. In this method, guide RNAs were used to target specific regions of human the *IBTK* gene, with the guide RNA sequences provided in Table 1. The Cas9 protein complexed with guide RNA were transfected into WT HEK293 cells using a SF cell line 4D-Nucleofector X kit (Lonza Cat No V4XC-2012) and 4D-Nucleofactor system with X unit (Lonza). For the mock transfection only Cas9 protein was transfected without any guide RNA in the WT HEK293 cells. Mixed pools of HEK293 IBTK α KO cells, IBTK α Δ SL cells, and WT counterparts were further expanded in culture, and the knock-out efficiency were calculated by isolating genomic DNA that was used as a template to amplify the indel portion by PCR using primers specific for the *IBTK* edited region. The Inference of CRISPR edits (ICE) software available on the Synthego website (98) was used to calculate the percentage of indels in the HEK293 IBTK α KO and IBTK α Δ SL pooled cells relative to WT control cells.

Stable HEK293T cells constitutively expressing FLAG-IBTK α under the control of CMV promoter were created by integrating the expression cassette into the genome. The HEK293T cells used for generating a stable cell line have a flippase recognition target (FRT) site integrated at the safe harbor locus of *AAVSI* gene. The FRT inserted HEK293T cells were co-transfected with donor plasmid expressing full length IBTK α tagged with FLAG at N-terminal and plasmid expressing flip recombinase. The flip recombinase enzyme drives recombination event between two FRT sites- the one present on the *AAVSI* gene and the second present on the donor plasmid with *IBTK α* expression cassette. This strategy led to the insertion of the expression cassette at the FRT site in *AAVSI* locus stably expressing FLAG-IBTK α under the control of CMV promoter. The stably expressing FLAG-IBTK α HEK293T cells were selected and further expanded in culture and FLAG-IBTK α protein expression was verified by immunoblot measurements. Furthermore, protein lysates were prepared from control WT, IBTK α KO, IBTK α Δ SL, and FLAG-IBTK α overexpressing cells and the levels of IBTK α protein were measured by immunoblot analyses as described below.

Table 1. List of *IBTK* α guide sequences and primer sequences

CRISPR guides targeting human <i>IBTK</i> gene		
	Target	Guide Sequences
1	IBTK α -Guide1	TTTGATGTGCAGTCAGGCAT
2	IBTK α -Guide2	CTTTGATGTGCAGTCAGGCA
3	IBTK α -Guide3	CGACACTTTGATGTGCAGTC
4	IBTK α -Guide4	GACATCCAAAGCATGCTTCA
CRISPR guides targeting SL region of human IBTKα 5'-leader		
	Target	Guide Sequences
1	IBTK α -SL-Guide1	TCCTGGAGTCAAGCACCAAG
2	IBTK α -SL-Guide2	AAAAGGGTCAGACAGTGTGG
Primers for sanger sequencing of genomic DNA		
	Target	Primer Sequences
1	IBTK α -gDNA-FP	AGGTCACCCTTGCAATTATGGATA
2	IBTK α -gDNA-RP	ATCCACTCCTTTCTGAATAAGCCA
RT-qPCR primers		
	Target	Primer Sequences

1	IBTK α -FP	CCGCCTTCCAGTTGTAATG
2	IBTK α -RP	AGCAAACAACCCAGTTGTCC
3	Firefly Luciferase-FP	CCAGGGATTTCAGTCGATGT
4	Firefly Luciferase-RP	AATCTCACGCAGGCAGTTCT
5	GAPDH-FP	AGGGCTGCTTTTAACTCTGGT
6	GAPDH-RP	CCCCACTTGATTTTGGAGGGA

2.2 Immunoblot analyses

For immunoblot analyses, 2.5×10^6 WT, IBTK α KO, and IBTK α Δ SL HEK293 cells were seeded in a 10 cm tissue culture dish (Corning, Cat No 353003) and cultured in complete DMEM media. Cells were grown to about 70% confluency and then treated with 1 μ M thapsigargin (Tg) (Sigma-Aldrich Cat No T9033) or vehicle DMSO (Thermo Fisher Scientific, Cat No BP-231-100). Following 8 hours of treatment, cell lysates were prepared by using 120 μ l of RIPA buffer solution supplemented with Halt protease and phosphatase inhibitors (Thermo Fisher Scientific, Cat No 78440) and 1 mM DTT. Cells were removed from the dish using a cell scraper and protein lysates were collected in 1.5 ml microfuge tubes and sonicated with 10 pulses while on ice. Lysates were then clarified by centrifugation at 12,000 rpm at 4°C with an Eppendorf centrifuge (5425 R). Protein concentrations were measured using DCTM protein assay kit (Bio-Rad, Cat No 5000112) according to the manufacturer's protocol. Protein samples were prepared in Laemmli protein sample solution (Bio-Rad, Cat No 1610747) with a final concentration of 1 μ g/ μ l and 20 μ g of each were separated by electrophoresis in a SDS polyacrylamide gel. Measurements of IBTK α protein used Bio-Rad 4-15% Mini protean TGX stain free precast protein gels (Cat No 4568084), while other proteins measured used 10% SDS polyacrylamide gels. After transferring the proteins to filters, immunoblot measurements were carried out using the following primary antibodies: IBTK α (1:1000, Thermo Fisher Scientific Cat No PA5-24224), ATF4 (1:1000, In-house (52)), CHOP (DDIT3) (1:500, Abcam Cat No ab11419), total eIF2 (1:3000, CST Cat No 5324S), p-eIF2 α (1:500, Abcam Cat No ab32157), GADD34 (1:2000, Proteintech Cat No 10449-1-AP), beta-actin (1:10000, Sigma-Aldrich A5441). Following washes in TBS solution supplemented with

0.1% tween 20, targeted proteins on the filters were visualized using the respective HRP-conjugated secondary antibody in combination with Bio-Rad Clarity Western ECL substrate (Cat No 1705060). Images were attained via a Bio-Rad ChemiDoc Imaging System. IBTK α immunoblots were quantified by Image J (99) and the relative levels of IBTK α among the samples were calculated with actin serving as a normalizing control. At least three biological replicates were carried out for immunoblot analyses.

2.3 Plasmid constructions

Two cDNA segments- one encoding the 550-nt long 5'-leader sequence along with the first 8 codons of the human *IBTK α* gene transcript that were fused in-frame to the second codon encoding the firefly luciferase CDS were inserted between HindIII and XhoI restriction site in pcDNA5 plasmid using the infusion cloning kit from Takara (Cat No 638947). The resulting P_{CMV}-IBTK α -Luc translational reporter contains the 5' leader sequence of *IBTK α* and CDS of *IBTK α* fused in-frame to luciferase downstream of constitutive CMV promoter. The P_{CMV}-IBTK α -Luc reporter was transiently transfected into HEK293T cells and luciferase assays were performed as described below. Similarly, P_{CMV}-ATF4-Luc reporter plasmid was constructed that contains the 5'-leader and CDS of mouse *ATF4* transcript fused in-frame to luciferase downstream of constitutive CMV promoter in pcDNA5 vector. The WT IBTK α and ATF4 luciferase reporters were used as templates to construct the mutant versions described in the Table 2. Mutations and insertions in the 5'-leader were created using GBlock segments featuring the cDNAs encoding the 5'-leaders or via site directed mutagenesis using the NEB Q5 site-directed

mutagenesis kit (Cat No E0554S). Each of the luciferase reporters were verified by Sanger Sequencing.

Table 2. List of different IBTK α -Luc and ATF4-Luc reporters

Gene Construct	Description of mutation
Reporters in Figure 10B	
IBTK α -CDS-Luc	550-nt long 5'-leader of Human <i>IBTKα</i> along with first 8 codons of IBTK α and firefly luciferase inserted between HindIII and XhoI site in pcDNA5 vector
IBTK α -uORF1-Luc	uORF1 fused in-frame to Luc CDS from the 19 th codon of uORF1
IBTK α -uORF2-Luc	uORF2 fused in-frame to Luc CDS from the 3 rd codon of uORF2
IBTK α -uORF3-Luc	uORF3 fused in-frame to Luc CDS from the 7 th codon of uORF3
IBTK α -uORF4-Luc	uORF4 fused in-frame to Luc CDS from the 12 th codon of uORF4
Reporters in Figure 12A-derived from IBTKα-CDS-Luc	
IBTK α - Δ uORF1	Initiation codon ATG to <u>AGG</u> of uORF1
IBTK α - Δ uORF2	Initiation codon ATG to <u>AGG</u> of uORF2
IBTK α - Δ uORF1+2	Initiation codon ATG to <u>AGG</u> of uORF1 and uORF2
IBTK α - Δ uORF3	Initiation codon ATG to <u>AGG</u> of uORF3

IBTK α - Δ uORF4	Initiation codon ATG to <u>AGG</u> of uORF4
IBTK α - Δ uORF3+4	Initiation codon ATG to <u>AGG</u> of uORF3 and uORF4
Reporters in Figure 12B-derived from IBTKα-uORF2-Luc	
IBTK α - Δ uORF1- uORF2-Luc	Initiation codon ATG to <u>AGG</u> of uORF1 in IBTK α -uORF2-Luc
Reporters in Figure 13A-derived from IBTKα-CDS-Luc	
IBTK α - Δ SL 232-260	Deletion of RNA stem loop sequence AGTGTGGAGGGGGAGTCCCCTCCTCACT
IBTK α -Heterologous SL	Substitution of AGTGTGGAGGGGGAGTCCCCTCCTCACT with CTGCAGTGGTGGAGCTTCCACCACTGCAG
Reporters in Figure 13B-derived from IBTKα-CDS-Luc	
IBTK α - Δ uORF1+2+3+4	Initiation codon ATG to <u>AGG</u> of uORF1, uORF2, uORF3, and uORF4
IBTK α - Δ uORF1+2+3+4 + Δ SL	Initiation codon ATG to <u>AGG</u> of uORF1, uORF2, uORF3, and uORF4 along with deletion of SL sequence AGTGTGGAGGGGGAGTCCCCTCCTCACT
Reporters in Figure 14-derived from IBTKα-CDS-Luc	
IBTK α - Δ uORF2+ Δ SL 232-260	Initiation codon ATG to <u>AGG</u> of uORF2 along with deletion of SL sequence AGTGTGGAGGGGGAGTCCCCTCCTCACT

IBTK α +50nt insert	Insertion of TACTATTATTTATCTTTGATTGTATCCATATGCCAACGG AAAGACCCTCT 3' of AAGGGTCAGAC
Reporters in Figure 15-derived from IBTKα-CDS-Luc	
IBTK α +100nt insert	Insertion of AAGTGCTAAATGAGTGAGTAACAGATTGTAGTACATG ATTAAGTAGTAACTAGAGAAATAAATCGAACCGACAT TTTCAATTTAGAGAGACTGCAGCATA 3' of AAGGGTCAGAC
Reporters in Figure 16A-derived from IBTKα-ΔSL 232-260	
IBTK α -GADD34 21nt+ Δ SL 232-260	Substitution of 21nt from the 3 rd codon of uORF2 in IBTK α - Δ SL 232-260 ATTTAAAAGGGTCAGACCCCC with GADD34 21nt surrounding uORF2 start codon CCCCCGGGGTGACGTGCAGCC
IBTK α - Δ uORF2+GADD34 21nt+ Δ SL 232-260	Initiation codon ATG to <u>AGG</u> of uORF2 in IBTK α -GADD34 21nt+ Δ SL 232-260
Reporters in Figure 16B-minimal IBTKα reporter	
IBTK α -uORF2+SL	Minimal IBTK α -Luc reporter featuring only uORF2 and SL upstream of the Luc CDS

IBTK α - Δ SL	Deletion of RNA stem loop sequence in minimal IBTK α -uORF2+SL AGTGTGGAGGGGGAGTTCCCCTCCTCACT
IBTK α - Δ uORF2	Initiation codon ATG to <u>AGG</u> of uORF2 in minimal IBTK α -uORF2+SL
IBTK α -GADD34 21nt+ Δ SL	Substitution of 21nt from 3 rd codon of uORF2 in minimal IBTK α - Δ SL ATTTAAAAGGGTCAGACCCCC with GADD34 21nt surrounding uORF2 start codon CCCCCGGGGTGACGTGCAGCC
IBTK α - Δ uORF2+GADD34 21nt+ Δ SL	Initiation codon ATG to <u>AGG</u> of uORF2 in minimal IBTK α -GADD34 21nt+ Δ SL
Reporters in Figure 17	
ATF4-CDS-Luc	594-nt long 5'-leader of Mouse <i>ATF4</i> along with first 2 codons of ATF4 and firefly luciferase inserted between HindIII and XhoI site in pcDNA5 vector. The initiation codon ATG of uORF2 mutated to <u>AGG</u> .
ATF4-IBTK α SL	Substitution of ATF4 CCTGCGGCAGCGTTGGCCTTTGCAGCGGCGGCAGC with IBTK α SL region GACAGTGTGGAGGGGGAGTTCCCCTCCTCACTCCC

ATF4-ΔuORF1+IBTKα SL	Initiation codon ATG to <u>AGG</u> of uORF1 in ATF4-IBTKα SL
-------------------------	--

2.4 Luciferase reporter assays

For luciferase report assays, six well culture plates (Corning Cat No 3516) were coated with Poly-D-lysine (PDL) from Sigma-Aldrich (Cat No P6407). 700 μ l of a solution of 10 μ g/ml PDL was added per well and the plate was then incubated for 20 minutes at room temperature. Following incubation, the PDL was aspirated out of the plates, and the wells were washed with sterile culture grade water. The plates were dried for 1.5 hours by partially keeping the lid open in the culture hood. Next, 2×10^5 HEK293T cells were seeded per well. The following day, WT, and mutant versions of IBTK α firefly luciferase reporters were co-transfected with pNL1.1-PGK-Nanoluciferase (Promega Cat No N1441) with the ratio of 1:100, respectively, using FuGENE 6 transfection reagent (Promega Cat No E2691). For each luciferase reporter, two plates of cells were transfected, one plate was used for collecting cell lysate for luciferase assay and one was used for RNA isolation for qPCR measurements of the reporter mRNA. Post 24 hours of transfection (day 3), cells were treated with 0.1 μ M Tg or 2 μ M PERK inhibitor GSK2656157 (84) or DMSO vehicle for 6 hours. Following treatment, media was removed by aspiration from the plates, and cells were washed with PBS solution. 500 μ l of 1X passive lysis buffer solution (Promega Cat No E1941) was then added to each well to collect cell lysates for the luciferase assays. Plates were placed on an orbital shaker at 100 rpm for 15 minutes to ensure cell lysis. At least three biological replicates were carried out for each luciferase assay. Cell lysates were transferred to 1.5 ml microfuge tubes. After clarifying lysates by centrifugation, 20 μ l of the supernatant was used for measuring firefly luciferase and Nano luciferase values using a luminometer. The firefly and nano luciferase values were determined and the firefly to nano luciferase

ratios were calculated for each. The firefly to nano luciferase ratio of vehicle treated WT IBTK α -Luc group was adjusted to 1 and served as the non-stressed control. The fold change for each the other groups were calculated by normalizing their firefly to nano luciferase ratios to that of DMSO treated WT IBTK α -Luc control group.

2.5 Polysome profiling and sucrose gradient ultracentrifugation

2.0 x 10⁶ WT HEK293 cells were seeded in 10 cm culture dish and on the next day cells were treated with 1 μ M Tg or vehicle DMSO for 6 hours. 30 minutes prior to the harvesting, cells were treated with 50 μ g/ml cycloheximide. Cells were collected and washed with cold PBS solution containing 50 μ g/ml cycloheximide and then 500 μ l of polysome lysis solution (20 mM Tris pH 7.5, 100 mM NaCl, 10 mM MgCl₂, 0.4% Nonidet P-40, and 50 μ g/ml cycloheximide) was added per 10 cm dish to lyse the cells. Cell lysates were prepared from the culture dishes with a cell scraper and placed into microfuge tubes. Lysates were then sheared with a sterile syringe and a 23-gauge needle and clarified by centrifugation at 10,000 x g for 15 minutes. Next, 400 μ l volume of the clarified supernatant was layered onto the top of a 10-50% sucrose gradient, followed by ultracentrifugation at 38,000 rpm using a Beckman SW41Ti rotor for 2 hours at 4°C. Fractionation of the sucrose gradient was carried out as previously described (28,100) using a Piston Gradient Fractionator (Biocomp) and a 254-nm ultraviolet monitor and Data Quest software were used to monitor the polysome profile. A total of 12 fractions were collected from each sample, which were combined pairwise for a total of six fractions.

To measure a shift in *IBTK α* , *ATF4*, and *GADD34* mRNA in the polysome fractions in response to Tg treatment, 3 μ l of 10 ng/mL firefly luciferase control RNA (Promega Cat No L4561) was spiked into each pooled sample to ensure for PCR normalization between fractions. 750 μ l of Trizol LS (Thermo Fisher Scientific Cat No 10296010) was added per 250 μ l of pooled sample and RNA isolation and cDNA generation was performed as mentioned detailed in the RNA isolation and RT-qPCR methods section below.

The percent total gene transcript in the polysome fractions was calculated as described previously (28,100). Briefly, the percentage shift in *IBTK α* , *ATF4*, and *GADD34* mRNA was calculated as (percentage total mRNA in fractions 5–6 during ER stress/the total mRNA levels) – (percentage total mRNA in fractions 5–6 during no stress/the total mRNA levels). The polysome to monosome ratio was calculated by measuring area under the curve of the polysome trace. The polysome fraction is defined as the portion of the trace that contains the trisome peak and all peaks after that.

2.6 RNA isolation and RT-qPCR

To measure the levels of *IBTK α* mRNA, HEK293 WT and *IBTK α* Δ SL cells were treated with Tg or DMSO for 6 hours and total RNA was collected using Qiagen RNeasy kit (Cat No 74104) according to manufacturer's protocol. To determine the levels of luciferase reporter mRNA, total RNA was collected from Tg or DMSO treated HEK293T cells that were transfected with different *IBTK α* or *ATF4* -driven reporters using TRIzol (Thermo Fisher Scientific Cat No 15596026) according to the manufacturer's protocol. At least three biological replicates were conducted for each

measurement. The concentration of RNA for all the samples were measured using a Nano drop spectrophotometer (Thermo Fisher Scientific). A total of 1µg of RNA was used for cDNA synthesis using High-Capacity cDNA Reverse Transcription kit (Thermo Fisher Scientific, Cat# 4368813) according to manufacturer's protocol. Following cDNA synthesis, samples were diluted five-fold with molecular biology grade water. 5µl was used from a total 200 µl diluted cDNA per well to perform the qPCR. The PCR amplification was carried out by PowerUp SYBR Green master mix (Thermo Fisher Scientific, Cat# A25742) using Applied Biosystems QuantStudio 5 Real-Time PCR system. The primers specific for the targets are mentioned in the Supplemental Table 1. The relative abundance for each transcript was calculated by $\Delta\Delta CT$ method with GAPDH serving as an internal control.

2.7 Statistical analysis

Values represent the mean +/- standard deviation and indicate at least three biological replicates. Two-way analysis of variance (ANOVA) or one-way ANOVA followed by a post hoc Tukey's multiple comparison test or honestly significant difference (HSD) test was used to analyze differences between multiple groups. P values less than 0.05 were considered statistically significant.

CHAPTER 3. RESULTS

3.1 Multiple regulatory elements are present in the 5'-leader of human *IBTK α* mRNA

IBTK α was previously identified in a high-throughput screen for mouse gene transcripts that are preferentially translated in response to ER stress (28). A phylogenetic comparison of the 5'-leader of the *IBTK α* showed that there are four upstream uORFs present in human and rodent mRNAs, with the 5'-proximal uORF1 and uORF2 broadly conserved among mammals (Figure 7A). Informatic comparisons of these *IBTK α* gene transcripts revealed that another conserved feature shared among the 5'-leaders is a RNA secondary stem-loop structure of $\Delta G^\circ = -20$ kcal/mol that is situated 11 nucleotides downstream of the uORF2 (Figures 7A and 7B). To address the mechanisms regulating human *IBTK α* expression during the ISR and the importance of the stem-loop structure (designated SL) and the uORFs in the translational control of human *IBTK α* , the SL was deleted in the *IBTK α* gene in human HEK293 cells using CRISPR/Cas9. The wild-type (WT) and SL-deleted cells (Δ SL) were treated with the ER stress agent thapsigargin (Tg) or vehicle and levels of *IBTK α* protein were measured by immunoblot (Figure 7C). Upon ER stress, WT cells showed enhanced levels of *IBTK α* protein that was accompanied by induced amounts of the ISR effectors ATF4, CHOP, and GADD34. By comparison, the Δ SL cells showed elevated levels of *IBTK α* protein independent of stress. Consistent with prior reports that *IBTK α* gene transcription is induced by ATF4 in the ISR (28), there were similar levels of increased *IBTK α* mRNA as judged by RT-qPCR in both the WT and Δ SL cells upon ER stress (Figure 7D). These results show that expression of

IBTKα is induced by stress and ablation of the SL leads to higher amounts of *IBTKα* protein expression independent of the stress conditions. The antibody validation of *IBTKα* was carried out by immunoblot measurements by using lysates prepared from *IBTKα* KO cells treated with Tg or vehicle and *IBTKα* overexpressing cells (Figure 8).

Next, polysome profiling was used to address translational control of *IBTKα*. WT HEK293 cells were treated with Tg or vehicle and lysates were prepared and subjected to sucrose gradient centrifugation to separate well translated heavy polysomes from monosomes and free ribosomes. ER stress and accompanying p-eIF2 α lowered translation initiation as viewed by a reduction in heavy polysomes (Figure 9A). Measurements of human *IBTKα* mRNA in the sucrose gradient fractions showed a shift towards heavy polysomes during ER stress, indicative of preferential translation during bulk translation repression (Figure 9B). This shift towards heavy polysomes in response to ER stress was similar to *ATF4* and *GADD34* mRNA (Figures 9C and 9D), two targets known to be subject to transcriptional and translational induction during the ISR. These results support the idea that *IBTKα* is subject to preferential translation in the ISR.

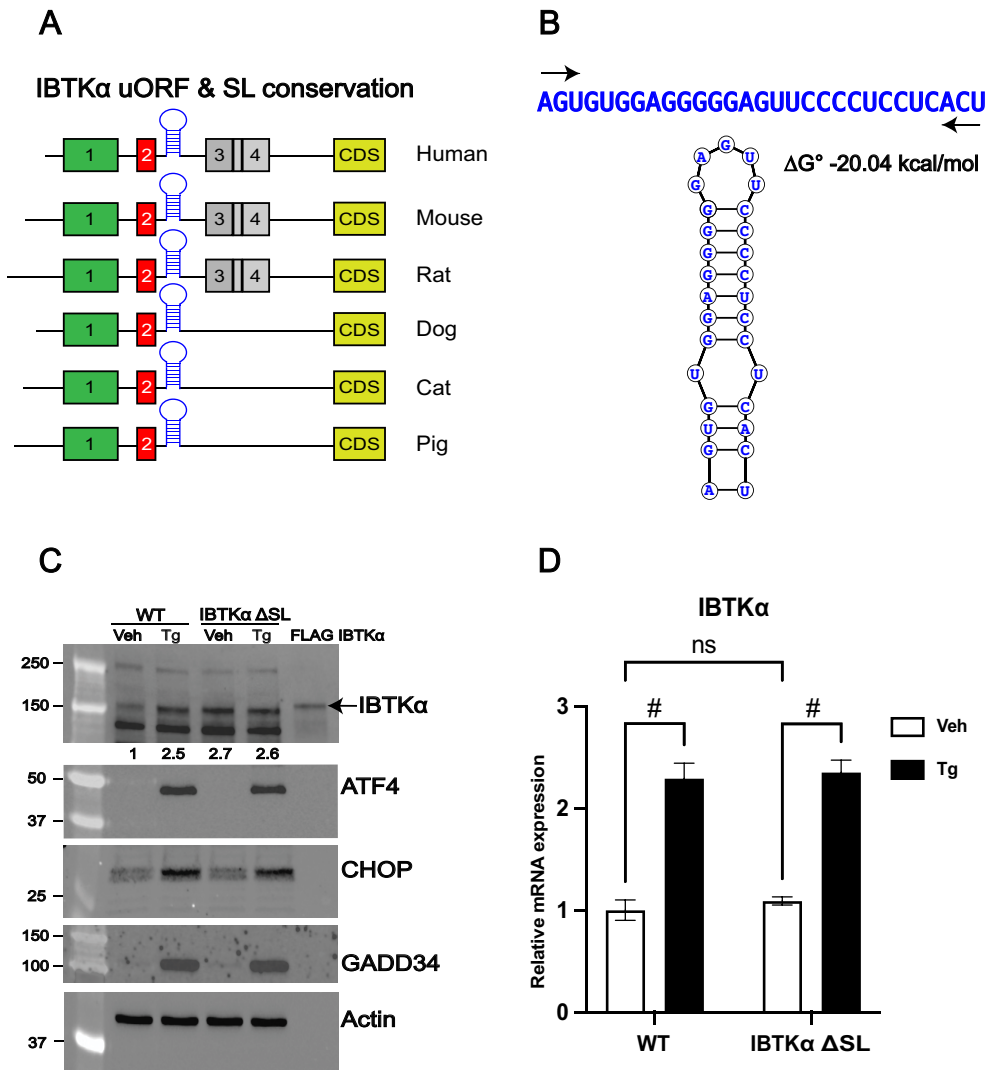


Figure 7. Conserved SL of human *IBTK α* mRNA is important for its translational control.

(A) Schematic representation of phylogenetic conservation of *IBTK α* uORFs and RNA SL among different mammalian species. Boxes indicate the uORFs 1-4 and the *IBTK α* CDS for organism. The SL is indicated downstream of uORF2. The given species include human, mouse, rat, dog, cat, and pig. The *IBTK α* 5'-leader sequences of the given species were aligned using a web based multiple sequence alignment program Clustal Omega

(101,102) (B) Sequence of conserved SL in the *IBTK α* mRNA, along with a schematic of SL structure. The structure and the free energy values of SL were calculated using a web-based Vienna RNA secondary structure prediction software (103). (C) WT and *IBTK α* Δ SL versions of HEK293 cells were treated with Tg or vehicle DMSO for 8 hours and the levels of *IBTK α* , ATF4, CHOP, GADD34 and actin proteins were measured by immunoblot analyses. Lysates containing a FLAG-tagged *IBTK α* was used as a maker in the immunoblot assay. Fold change for *IBTK α* relative to WT vehicle is indicated at the bottom of the *IBTK α* panel. (D) WT HEK293 and *IBTK α* Δ SL cells were treated with Tg or vehicle for 8 hours and cDNA was generated after collecting total RNA. Levels of *IBTK α* mRNA were measured by RT-qPCR and are presented as a bar graphs that are normalized to WT cells treated with vehicle. One-way ANOVA with Tukey's HSD test. The symbol # is equal to p-value ≤ 0.0001 .

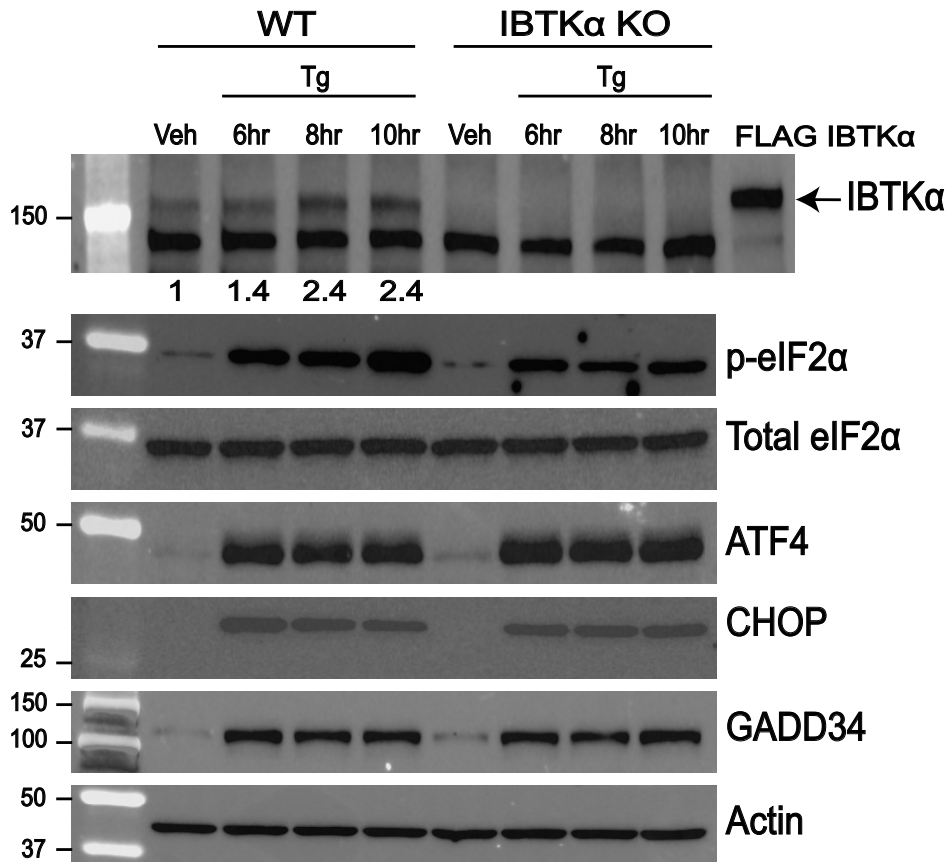


Figure 8. Validation of IBTK α antibody by immunoblot using HEK293 IBTK α KO cells.

HEK293 WT and IBTK α KO cells were treated with Tg or vehicle DMSO for 6, 8 and 10 hours and the levels of IBTK α , p-eIF2 α , total eIF2 α , ATF4, CHOP, GADD34 and actin proteins were measured by immunoblot analyses. Protein lysate collected from HEK293T expressing FLAG tagged IBTK α was used as a marker for probing IBTK α . Fold change for IBTK α relative to WT vehicle is indicated at the bottom of the IBTK α panel.

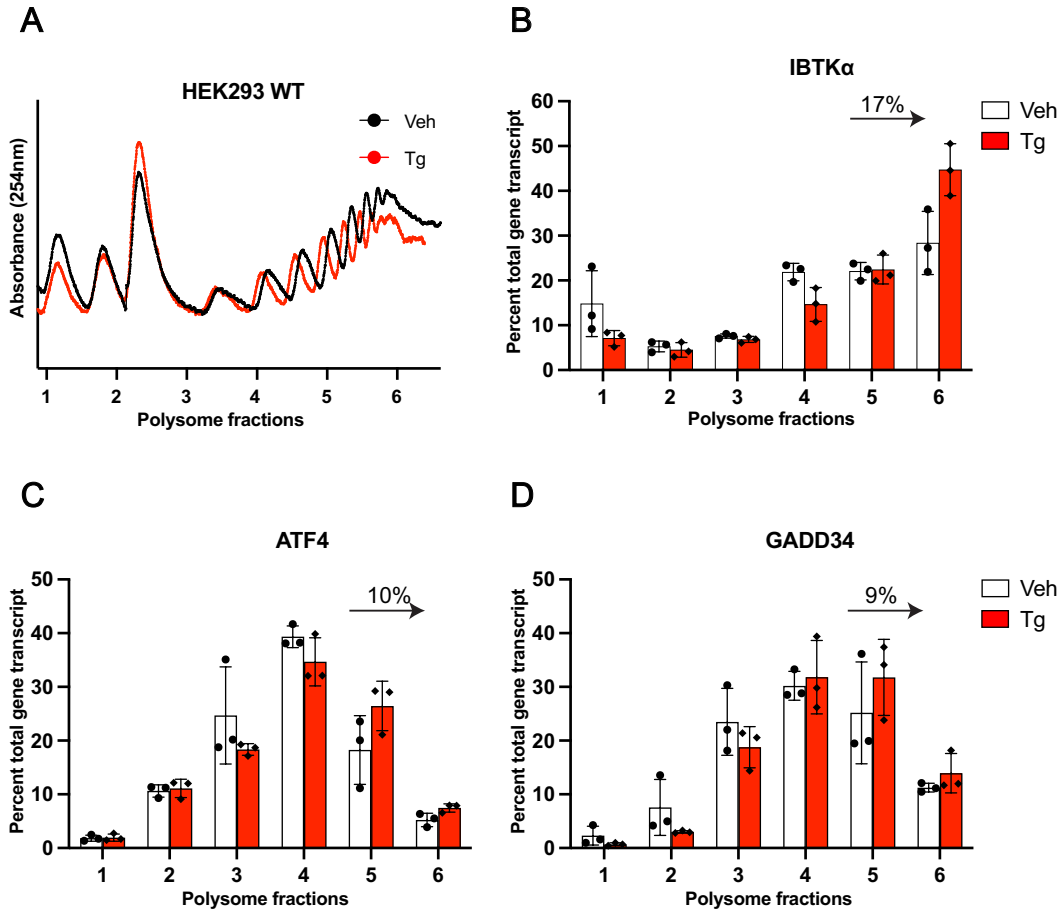


Figure 9. Human *IBTKα* mRNA shift towards polysomes during ER stress.

WT HEK293 cells were treated with Tg or vehicle DMSO for 6 hours and cell lysates were analyzed by polysome profiling. (A) The A_{254} of the profiles are shown, with free ribosomes, monosomes and polysomes indicated. The average polysome to monosome ratio of three biological replicates for vehicle or Tg treated group is 2.8 and 1.9, respectively. RNA was isolated from the indicated polysome fractions and the levels of *IBTKα* (B), *ATF4* (C), and *GADD34* (D) transcripts were measured from three biological replicates by RT-qPCR as described in the Experimental Procedures. The bar graphs

show the percentage of total *IBTK α* , *GADD34*, and *ATF4* mRNAs in each fraction and their shift towards heavy polysome during ER stress.

3.2 The uORF2 functions as a major inhibitory element in *IBTK α* translational control

To delineate the key regulatory elements directing the preferential translation of *IBTK α* , a translational reporter was constructed that contained a constitutive CMV promoter, the full-length *IBTK α* 5'-leader, and the firefly luciferase CDS (Figure 10A). This reporter designated P_{CMV}-*IBTK α* -Luc was transiently transfected into HEK293T cells in combination with a plasmid encoding nanoluciferase, to aid in normalization in this dual luciferase assay. Upon Tg treatment, the *IBTK α* -Luc activity was increased about 4-fold, with no significant difference in the reporter mRNA as judged by RT-qPCR (Figure 10B). It is noted that the nanoluciferase activity was consistently reduced by about 30% upon ER stress (Table 3). Nanoluciferase is a long-lived reporter, and the decrease reflects the bulk translation repression that occurs upon induced p-eIF2 α during ER stress. Therefore, the reduction in nanoluciferase accounts for a small portion, albeit measurable, of the increase in the measured induction of *IBTK α* -Luc in response to ER stress. As expected, the addition of a small molecule inhibitor of PERK, GSK2656157 (84), lowered P_{CMV}-*IBTK α* -Luc expression in response to Tg treatment, supporting the role of this eIF2 α kinase and the ISR in facilitating its translation (Figure 11). These results show that the *IBTK α* -Luc reporter can recapitulate key features of preferential translation observed during the ISR.

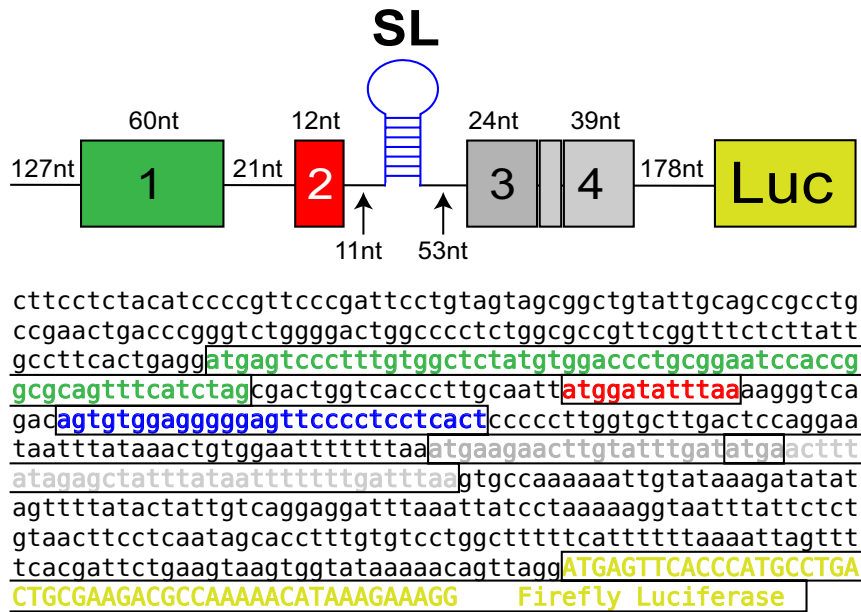
There are four uORFs in the human *IBTK α* mRNA and to determine whether each is translated, uORFs were directly fused in-frame to the firefly luciferase reporter. The uORF2 is robustly translated, with more modest translation of uORF1 and minimal translation of uORFs 3 and 4 (Figure 10B). These results are consistent with the

phylogenetic analysis showing that uORF1 and uORF2 are conserved among mammalian *IBTK α* genes. Next, the roles of each uORF in the *IBTK α* -Luc reporter expressing the full length 5'-leader (Figure 12A) was addressed. To eliminate the contribution of each uORF in *IBTK α* translation control, the encoded initiation codon ATG was substituted to AGG. Removal of uORF1 led to an inability to induce luciferase activity in response to ER stress (Figure 12A, panel b). By comparison, loss of uORF2 led to robust *IBTK α* -Luc expression even in the absence of ER stress (Figure 12A, panel c). These results suggest that uORF1 can be a positive acting element in *IBTK α* translational control, whereas uORF2 is a major inhibitory element. Given that there were high levels of luciferase activity when both uORF1 and uORF2 were mutated in the reporter that were independent of ER stress, the inhibitory uORF2 function is dominant in translational control (Figure 12A, panel d). This result also suggests that the role of uORF1 is in part to overcome uORF2. Loss of uORF3 and uORF4 individually or in combination did not significantly alter induction of luciferase activity in response to ER stress as compared to WT (Figure 12A, panels e, f, and g). These results are consistent with the minimal translation observed for uORFs 3 and 4 and indicates that these elements are not significant contributors to *IBTK α* translational control.

To determine whether the function of the 5'-proximal uORF1 can affect translation of the inhibitory uORF2, the uORF2 was fused in-frame to the luciferase CDS in the presence or absence of uORF1. There were high levels of uORF2-Luc activity which were further elevated upon elimination of uORF1 (Figure 12B, panels b and c). It is noted that upon ER stress, both reporters were further enhanced. However, mRNA measurements for these reporters were also increased during the stress treatments,

suggesting that increases in transcript levels were a contributor to this induction. These results suggest that part of the reason why the 5'-proximal uORF1 is a positive element is that ribosome translation of the element can in part thwart translation of the next uORF2, a major inhibitory element that is suggested to prevent reinitiation of translation at the downstream *IBTK α* CDS.

A



B

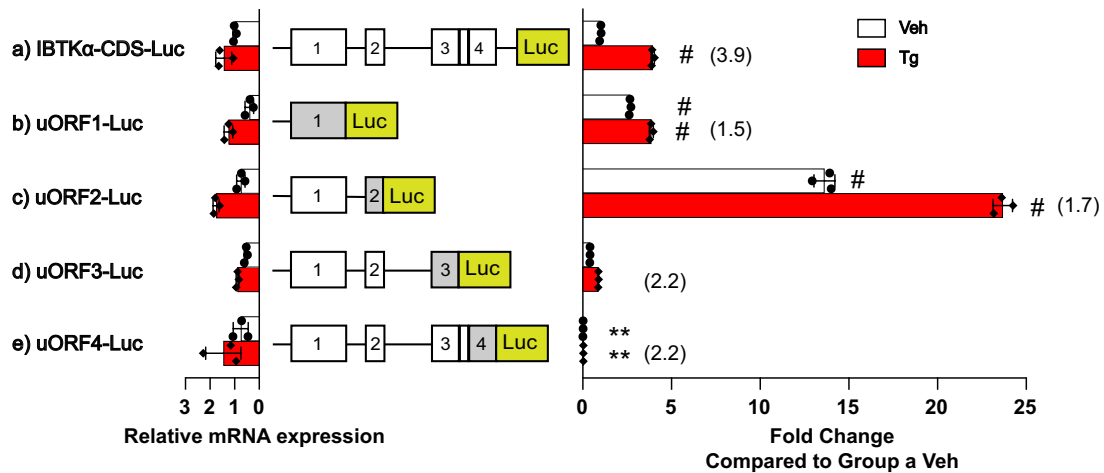


Figure 10. *IBTK α* mRNA is preferentially translated in response to ER stress.

(A) Schematic representation of the P_{CMV}-IBTK α -Luc reporter featuring the encoded 5'-leader of human *IBTK α* that was fused in-frame with the firefly luciferase CDS. The sequence of the 5'-leader IBTK α -Luc reporter is also shown with color coded uORFs and

the conserved SL sequence. (B) The P_{CMV}-IBTK α -Luc reporter was co-transfected with Nano luciferase reporter into HEK293T cells and treated with Tg or vehicle DMSO for 6 hours (panel a). Alternatively, the Luc CDS was fused in-frame to each of the four *IBTK α* uORFs and assayed in the dual reporter system in the presence or absence of ER stress (panels b-e). Each of the reporter constructs are illustrated in panel and Luc expression was measured by Dual Glo luciferase in stressed (Tg, red bars) or vehicle (Veh, white bars) cells. Bar graphs are shown for each reporter, with values normalized to the IBTK α -CDS-Luc reporter expressed in vehicle treated cells. Luciferase reporter mRNAs were also measured by RT-qPCR and are shown as bar graphs on the left side of the depicted reporter constructs. Three biological replicates are reported for each condition, with data points included in the bar graphs. The values in parentheses represents induction ratios within the same group determined as the ratio of Luc activity of Tg treated samples compared to vehicle treated. Two-way ANOVA with Tukey's HSD test. The symbol # is equal to p-value ≤ 0.0001 ; ** is equal to p-value ≤ 0.01 .

Table 3. Raw values of firefly and nano luciferase from HEK293T cells transfected with the WT version of P_{CMV}-IBTK α -Luc reporter and treated with thapsigargin or vehicle.

No.	Sample Name	Firefly Luciferase	Nano Luciferase	Ratio	Fold Change
1	HEK293T CMV IBTK WT UTR-Luc Veh-1	4535136	76491632	0.06	0.95
2	HEK293T CMV IBTK WT UTR-Luc Veh-2	4999304	77768904	0.06	1.03
3	HEK293T CMV IBTK WT UTR-Luc Veh-3	4393406	69304776	0.06	1.02
4	HEK293T CMV IBTK WT UTR-Luc Tg-1	12906654	53063924	0.24	3.90
5	HEK293T CMV IBTK WT UTR-Luc Tg-2	14121119	55876400	0.25	4.06
6	HEK293T CMV IBTK WT UTR-Luc Tg-3	13799587	56984420	0.24	3.89

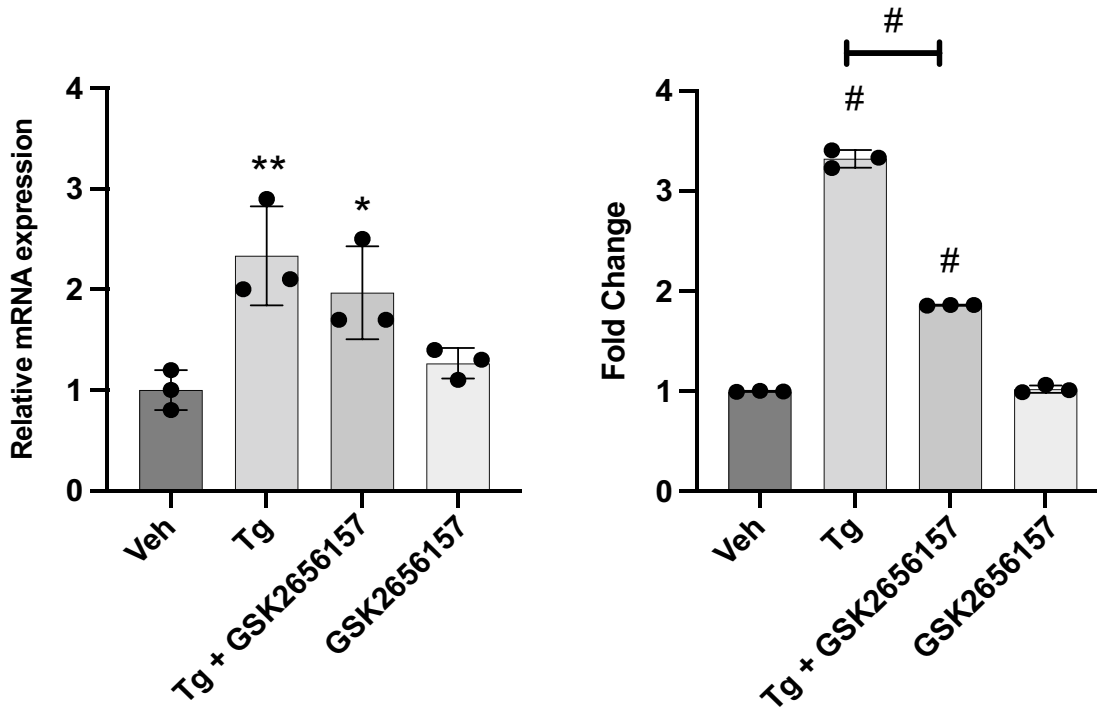
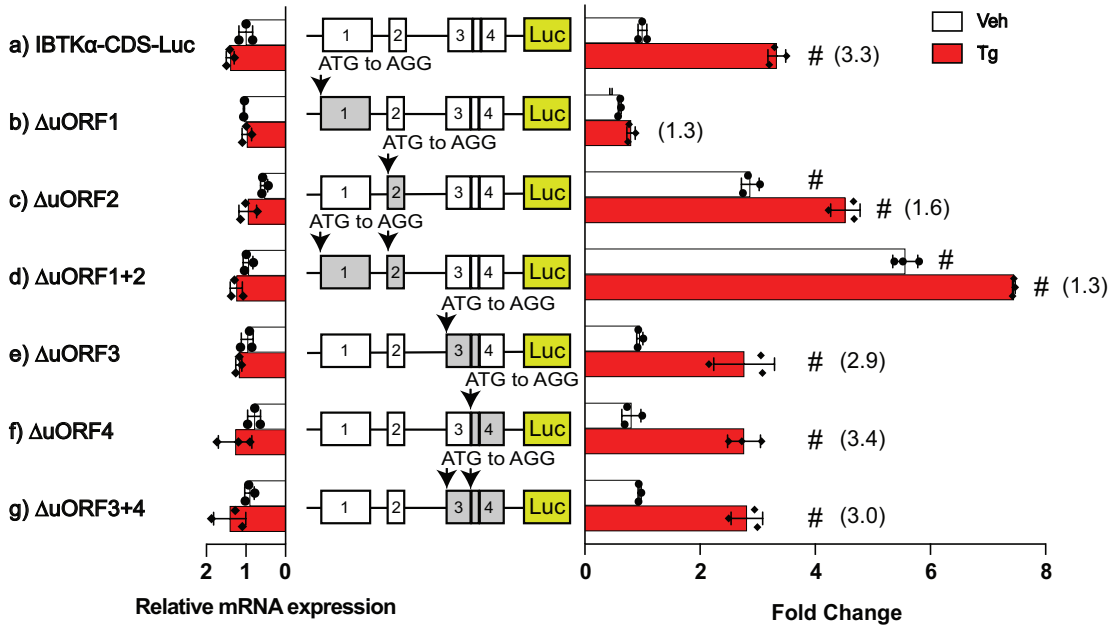


Figure 11. Preferential translation of *IBTK α* during ER stress is dependent on the activity of eIF2 α kinase PERK.

HEK293T cells were transfected with WT versions of P_{CMV}-*IBTK α* -Luc reporter and were treated with Tg, combination of Tg and PERK inhibitor GSK2656157 (84), GSK2656157 by itself or vehicle. Luciferase activity (right panel) and the corresponding luciferase mRNA (left panel) were measured and presented in the bar graphs that are normalized to the non-stressed cells. Three biological replicates are depicted in the bar graphs. One-way ANOVA with Tukey's HSD test. The * symbol is equal to p-value \leq 0.05, ** is equal to p-value \leq 0.01, # is equal to p-value \leq 0.0001.

A



B

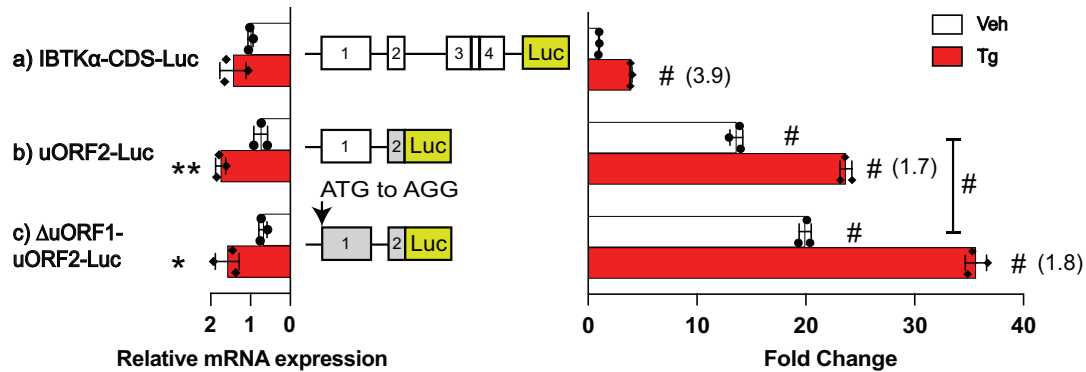


Figure 12. Translational control of *IBTK α* features an inhibitory uORF2.

(A) WT and the indicated mutant versions of P_{CMV}-IBTK α -Luc reporters were assayed in HEK293T cells and treated with Tg or vehicle DMSO for 6 hours. Elimination of the uORFs in the P_{CMV}-IBTK α -Luc reporters was carried out individually or in combinations by substituting the initiation codons ATG to AGG. Bar graphs show luciferase expression for each reporter and values normalized to the IBTK α -CDS-Luc reporter expressed in

non-stressed cells. Luc mRNAs were measured by RT-qPCR and are shown as bar graphs on the left side of the depicted reporter constructs. (B) Luc reporters were constructed with direct fusions of uORF2 with Luc CDS in the presence of intact uORF1 (panel b) or a version with the encoded uORF1 initiation codons changed from ATG to AGG (panel c). These reporters were transfected into HEK293T cells and treated with Tg or vehicle for 6 hours and bar graphs show luciferase expression for each reporter. Values are normalized to the IBTK α -CDS-Luc reporter expressed in non-stressed cells. Luc mRNAs were measured by RT-qPCR and are also shown as bar graphs. Three biological replicates are reported for each condition, with data points included in the bar graphs. Values in parentheses represent induction ratios for each reporter within the same group determined as the ratio of Luc activity of Tg treated samples compared to vehicle treated. Two-way ANOVA with Tukey's HSD test. The * symbol is equal to p-value ≤ 0.05 , ** is equal to p-value ≤ 0.01 , # is equal to p-value ≤ 0.0001 .

3.3 The SL functions in conjunction with uORF2 to regulate *IBTK α* translation

Prior analysis of genomic deletion of the SL embedded in the 5'-leader of *IBTK α* suggested that it has a repressive function in the translational control (Figure 7C). This idea was tested in the *IBTK α* -Luc reporter by targeted deletion of the SL element and viewed high levels of luciferase activity even in the absence of ER stress (Figure 13A, panel b). Inclusion of a heterologous stem-loop sequence of similar predicted stability ($\Delta G^\circ = -20$ kcal/mol) restored to near WT levels of regulation, suggesting a SL at this position is central for the *IBTK α* translation control (Figure 13A, panel c). Next, whether the SL by itself is a potent repressing element was addressed. Each of the four uORFs were eliminated in the *IBTK α* -Luc reporter, leaving only the SL element, resulting in a significant increase in expression compared to WT (Figure 13B, panel a compared to b). An analogous reporter was constructed that removed the four uORFs in combination with a deletion of the SL, leading to no significant difference in *IBTK α* -Luc compared to the reporter eliminating only the uORFs (Figure 13B, panel b compared to c). The conclusion from this experiment was that the SL by itself is not an appreciable inhibitor of ribosome scanning and *IBTK α* translation.

Next, it was important to determine whether the SL inhibitory function is derived from its proximity to the uORF2. As noted earlier, removal of uORF2 led to high levels of *IBTK α* -Luc expression even in the absence of stress (Figure 14, panel b). Deletion of the SL led to even further increase in luciferase activity (Figure 14, panel c) that was only modestly elevated with the combined deletion of both uORF2 and the SL. Together, these observations suggest that the two elements function in combination to inhibit the downstream *IBTK α* CDS translation (Figure 14, panel d). To address the proximity of the

SL to uORF2, the 5'-leader of the IBTK α -Luc reporter was adjusted such that the SL was 50 nucleotides further downstream of the uORF2 (Figure 14, panel e). Increasing the distance between the SL and uORF2 led to progressive higher levels of luciferase activity during the non-stressed conditions compared to WT, whereas the induced levels of IBTK α -Luc remained similar to WT during ER stress. Insertion of 100 nucleotides between the SL and uORF2 did not further enhance luciferase activity beyond that measured for the 50-nucleotide insertion (Figure 15). These results indicate that the proximity of the SL to the uORF2 is critical for their repressing functions in *IBTK α* translational control in basal conditions.

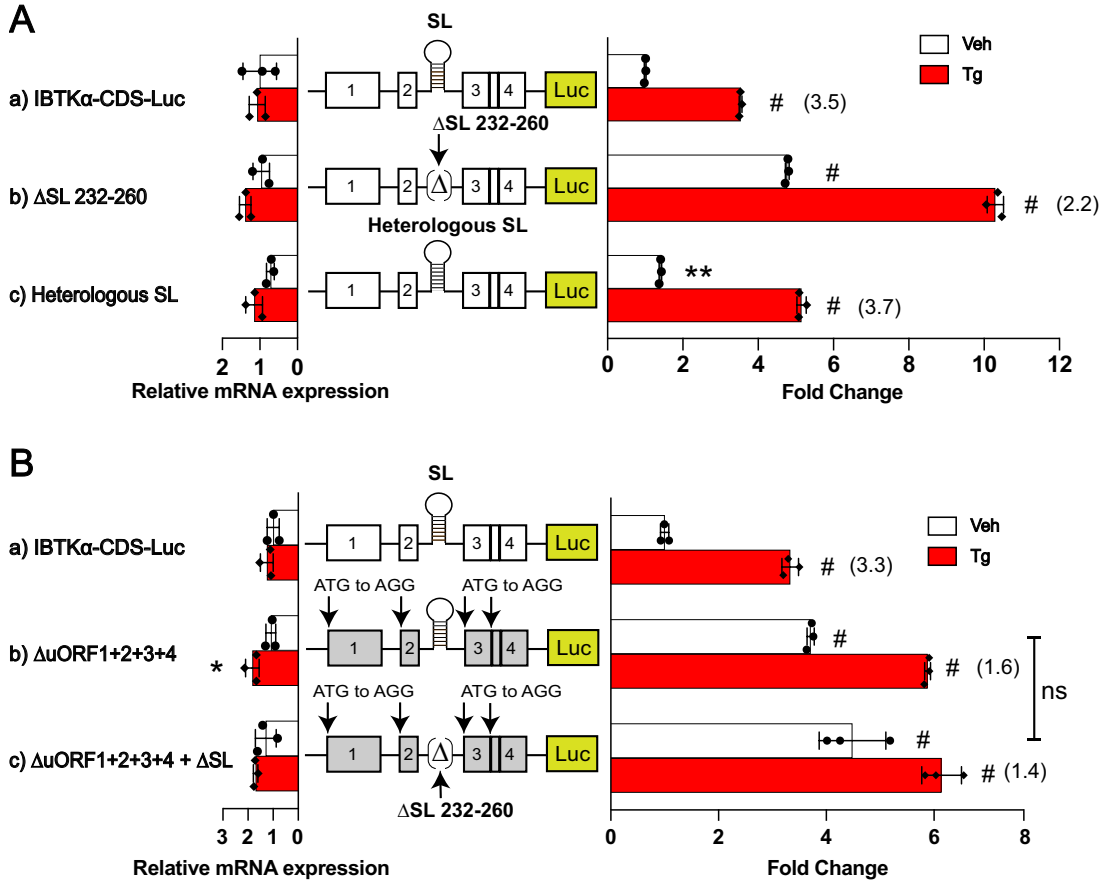


Figure 13. The conserved SL regulates *IBTK α* translation by functioning in conjunction with inhibitory uORF2.

(A) Mutant versions of P_{CMV}-IBTK α -Luc reporters were constructed that included deletion of SL sequence (panel b, Δ SL 232-260) and a reporter in which WT SL sequence was substituted with a heterologous SL sequence with similar ΔG° (panel c). WT and mutant IBTK α -Luc reporters were transfected into HEK293T cells and treated with Tg or vehicle DMSO for 6 hours. Luciferase activities are shown in bar graphs with corresponding Luc mRNA levels that were measured by RT-qPCR. Values are normalized to the IBTK α -CDS-Luc reporter expressed in non-stressed cells. (B) Mutant

versions of P_{CMV}-IBTK α -Luc reporters were constructed that had all four uORFs eliminated by mutation of the encoded start codons (panel b) or both loss of the uORFs in combination with deletion of the SL (panel c). Reporter plasmids were transfected into HEK293T cells and treated with Tg or vehicle for 6 hours. Luciferase activities and corresponding mRNA levels are shown for each reporter. Values are normalized to the WT IBTK α -Luc expressed in non-stressed cells. There are three biological replicates depicted in the bar graphs. For each group the induction ratios are determined in response to ER stress by taking the ratios of Luc activity of Tg treated samples compared to vehicle treated and are indicated in parentheses. Two-way ANOVA with Tukey's HSD test. The * symbol is equal to p-value ≤ 0.05 , # is equal to p-value ≤ 0.0001 .

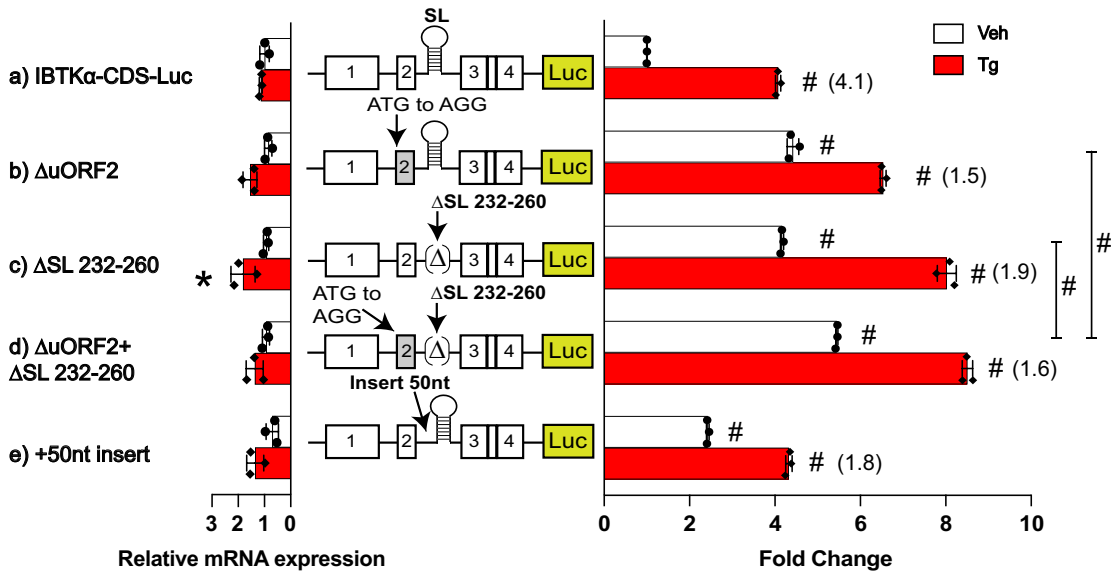


Figure 14. Conserved SL regulates *IBTK α* translation by contributing to the repressing function of uORF2.

WT and the indicated mutant versions of P_{CMV}-IBTK α -Luc reporters were transfected into HEK293T cells and treated with Tg or vehicle DMSO. Mutant versions of P_{CMV}-IBTK α -Luc reporter included mutation of uORF2, a deletion of the SL sequence and an insertion of a 50nt segment that extended the distance between the uORF2 stop codon and the SL. Luciferase activity and corresponding Luc mRNA were measured and presented in the bar graphs that are normalized to the WT IBTK α -Luc activity in non-stressed cells. Three biological replicates are depicted in the bar graphs, with values in parentheses indicating the ER stress induction for each group calculated by taking the ratio of Luc activity of Tg treated samples compared to vehicle treated. Two-way ANOVA with Tukey's HSD test. The * symbol is equal to p-value ≤ 0.05 , # is equal to p-value ≤ 0.0001 .

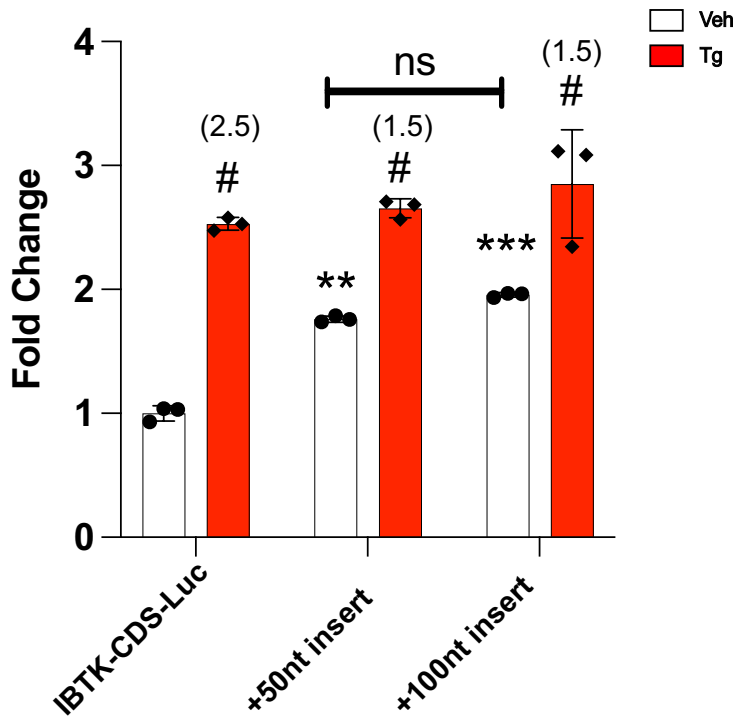


Figure 15. Distance between the SL and uORF2 is critical for translational control of *IBTKα*.

HEK293T cells were transfected with WT and the indicated mutant versions of P_{CMV}-IBTK α -Luc reporters and were treated with Tg or vehicle DMSO. Mutant versions of P_{CMV}-IBTK α -Luc reporter included an insertion of a 50nt or a 100nt segment that extended the distance between the uORF2 stop codon and the SL. Luciferase activity were measured and presented in the bar graphs that are normalized to the WT IBTK α -Luc activity in non-stressed cells. Three biological replicates are depicted in the bar graphs, with values in parentheses indicating the ER stress induction for each group calculated by taking the ratio of Luc activity of Tg treated samples compared to vehicle treated. Two-way ANOVA with Tukey's HSD test. The symbol # is equal to p-value \leq 0.0001 and ns represents non-significant.

3.4 The SL functions in conjunction with uORF2 to thwart translation reinitiation

Given that the SL contributes to the repressing functions of the uORF2, it was posited that the SL contributes importantly to the ability of uORF2 to thwart translation reinitiation at the *IBTK α* CDS. This idea was tested using two different reporter strategies. First, the SL was removed from the *IBTK α -Luc* reporter that led to elevated expression even in the absence of stress (Figure 16A, panel b). This idea supports the model that the SL functions to diminish ribosome reinitiation following translation of uORF2. Previous study determined that the encoded ProProGlyStop (PPG*) sequence in the uORF2 situated in the 5'-leader of *GADD34* is the basis for why it thwarts downstream translation reinitiation at the downstream CDS (67). In that study it was suggested that the altered termination of translation of the *GADD34* uORF2 lowered the ability of reinitiating ribosomes to be retained on the *GADD34* mRNA and resume scanning downstream for subsequent translation of the CDS (67). Of importance, the PPG* element is modular and can be substituted into other short uORFs to confer this repressing function (67). Following up on this idea, the PPG* was substituted into the uORF2 in the *IBTK α -Luc* devoid of the SL and determined that this substitution substantially lowered luciferase activity, consistent with lowered translation reinitiation (Figure 16A, panel c). Translation of the uORF2 in this reporter was essential for this regulation because an uORF2 containing the PPG* but devoid of an initiation codon led to elevated levels of luciferase activity independent of stress (Figure 16A, panel d).

The second reporter strategy for testing whether the SL contributes to the ability of the uORF2 to thwart reinitiation of translation involved a minimal *IBTK α -Luc* reporter featuring only the uORF2 and SL upstream of the Luc CDS (Figure 16B).

Removal of either the uORF2 or the SL led to significantly higher levels of luciferase activity compared to the WT version (Figure 16B, compare panels b and c to panel a). Consistent with the earlier experiment, substitution of the PPG* into the uORF2 in the reporter devoid of the SL showed only low levels of luciferase expression (Figure 16B, panel d). Furthermore, mutation of the initiation codon of the uORF2 containing the PPG* led to elevated levels (Figure 16B, panel e). Together these results suggest that either inclusion of the SL or the PPG* was important for uORF2 to confer impaired downstream reinitiation of translation.

Finally, to determine whether SL function is modular for inhibition of translation reinitiation, this element was tested with the uORF1 in *ATF4*. As described in the Introduction section 1.6, the *ATF4* uORF1 is a short coding sequence that is well translated and allows for efficient reinitiation of translation at the downstream coding sequence (53,57). In this reporter system, the repressing uORF2 was eliminated by mutation of the encoded initiation codon from ATG to AGG and relied on the ATF4-CDS for a measure of reinitiation (Figure 17). Substitution of the SL into the uORF1-Luc reporter significantly diminished luciferase activity (Figure 17, compare panels a and b). Removal of the uORF1 but retention of the SL sharply enhanced luciferase expression, indicating again that the SL by itself is not repressing, but rather its proximity downstream of uORF1 allows for the combined elements to thwart translation reinitiation. The conclusion from this experiment is that the SL is modular and can lower translation initiation when placed downstream in proximity with an uORF.

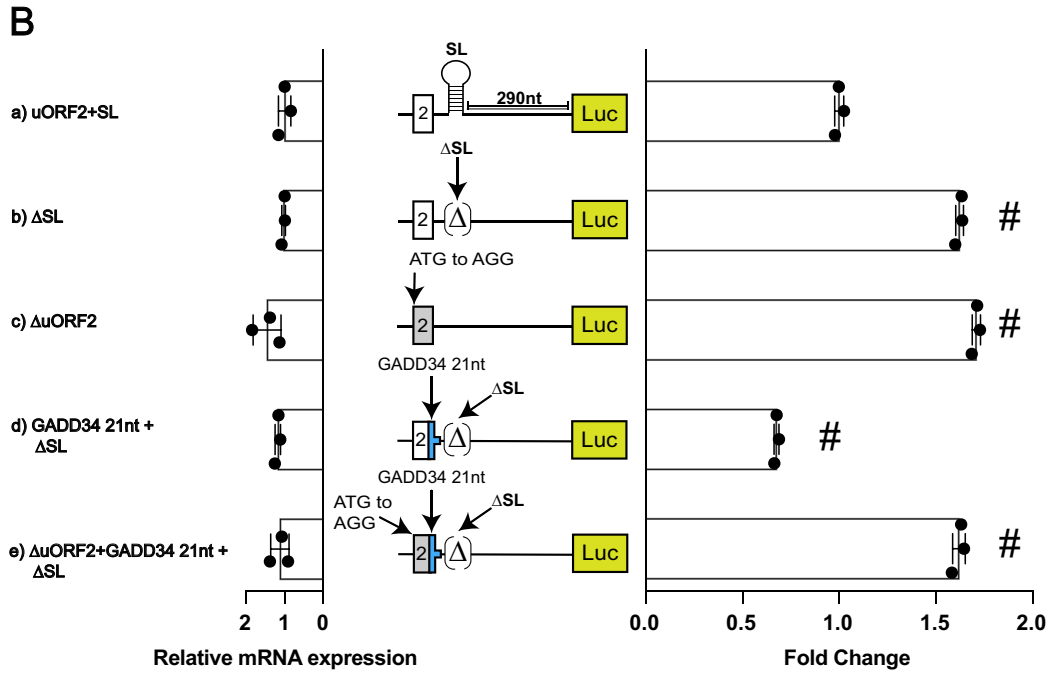
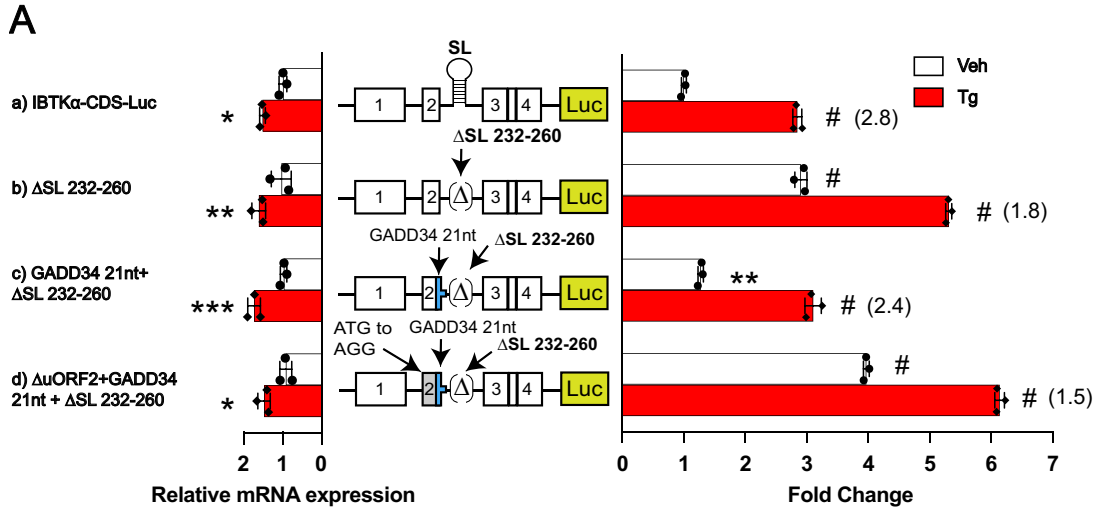


Figure 16. The SL and uORF2 regulates *IBTKα* translation by blocking translation reinitiation.

(A) WT and mutant versions of P_{CMV} -*IBTKα*-Luc reporters were transfected into HEK293T subjected to ER stress for 6 hours or no stress treatment. Mutant versions of the reporter that are illustrated included deletion of the SL sequence, along with

substitution of the corresponding residues from the 3rd codon of *IBTK α* uORF2 with the *GADD34* uORF2 encoding PPG*. Furthermore, mutation of initiation codon of uORF2 was included as indicated. Luciferase activities were measured, along with levels of Luc mRNA, and are presented in the bar graphs that are normalized to the WT *IBTK α* -Luc activity in cells not subjected to stress. Three biological replicates are depicted in the bar graphs and values in parentheses indicate the ER stress induction for each group calculated by taking the ratio of Luc activity of Tg treated samples compared to vehicle treated. (B) A minimal version of the P_{CMV}-*IBTK α* -Luc reporter featuring only the uORF2 and SL upstream of the Luc CDS was constructed as illustrated in panel a. Mutations were also prepared in the minimal *IBTK α* -Luc reporter that included deletion of the SL (panel b), elimination of the uORF2 (panel c), and substitution of the *GADD34* uORF2 encoding PPG* into the uORF2 in combination with the deletion of the SL with a functional uORF2 start codon (panel d) or with the ATG codon mutation changed to AGG (panel e). Luciferase activity and Luc mRNA activity were measured and presented in a bar that is normalized to the WT version (panel a). Two-way ANOVA with Tukey's HSD test for (A) and one-way ANOVA with Tukey's HSD test for (B). The * symbol is equal to p-value ≤ 0.05 , ** is equal to p-value ≤ 0.01 , *** is equal to p-value ≤ 0.001 , # is equal to p-value ≤ 0.0001 .

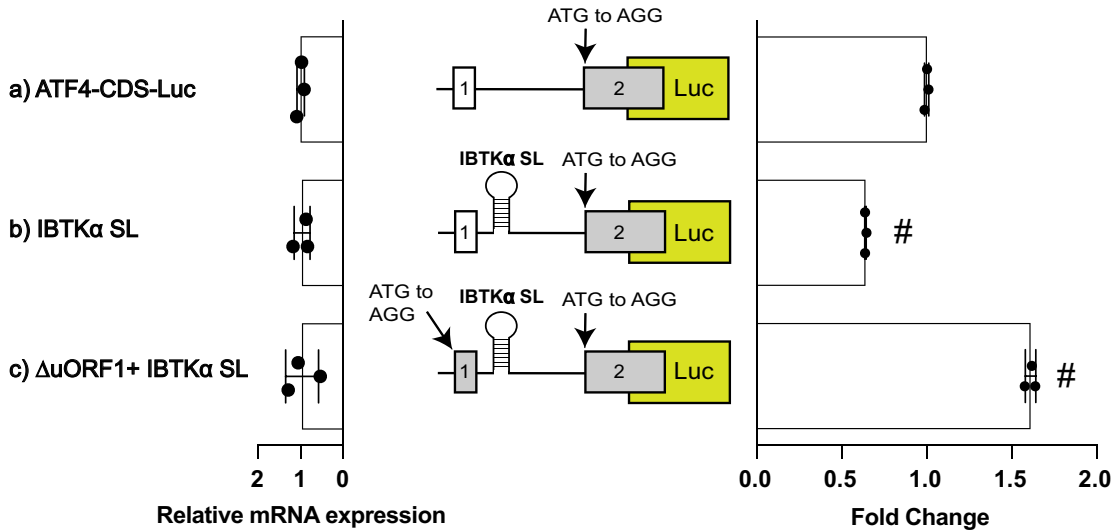


Figure 17. The property of *IBTKα* SL to block reinitiation is transferrable to heterologous system that contains 5' leader of mouse *ATF4*.

A P_{CMV}-ATF4-Luc reporter was constructed with mutation in the uORF2 start codon to AGG, resulting in the functional loss of this inhibitory uORF (panel a). The encoded *IBTKα* SL was inserted 11 nucleotides downstream of the ATF4 uORF1 (panel b) and a version of this heterologous reporter was constructed with an ATG to AGG substitution in the uORF1 (panel c). This collection of ATF4-Luc reporters was transfected into HEK293T cells and cells were cultured in the absence of stress. Luciferase activity and corresponding Luc mRNA levels were measured and are represented in a bar graph. Values are presented relative to the ATF4-Luc in panel a. One-way ANOVA with Tukey's HSD test. The symbol # is equal to p-value ≤ 0.0001 .

CHAPTER 4. DISCUSSION

4.1 Translational control of human *IBTK α*

This thesis addressed the processes contributing to the preferential translation of human *IBTK α* mRNA during ER stress. Among four canonical uORFs predicted in the 5'-leader of *IBTK α* , uORF2 was shown to be well translated and serve as a major inhibitory element that hinders translation reinitiation at the downstream *IBTK α* CDS. The polypeptide encoded by uORF2 is only three amino acids long and therefore by itself does not appear to be an efficient barrier of translation. Rather uORF2 functions in conjunction with a stem-loop structure that is just 11 nucleotides downstream and together these elements are critical for thwarting downstream ribosome reinitiation. Both the uORF2 and the SL are well conserved phylogenetically and the distance between them is critical for thwarting downstream ribosome reinitiation. Upon increasing the distance between the uORF2 and the SL an increase in luciferase activity was observed even in absence of stress compared to WT (Figures 14 and 15). This finding supports the idea that uORF2 and the SL work synergistically in *IBTK α* translational control. The *IBTK α* SL is modular and can be introduced downstream of the uORF1 in the *ATF4* mRNA to change it from an uORF that allows for efficient translation reinitiation to one that prevents downstream translation. Along with uORF2, *IBTK α* uORF1 is modestly translated and it is suggested to function antagonistically to uORF2, such that translation of uORF1 precludes initiation at the nearby uORF2 (model in Figure 18). These processes may be a contributor to the bypass of uORF2 that is suggested to occur in response to ER stress. These results indicate that the bar code conferring translational

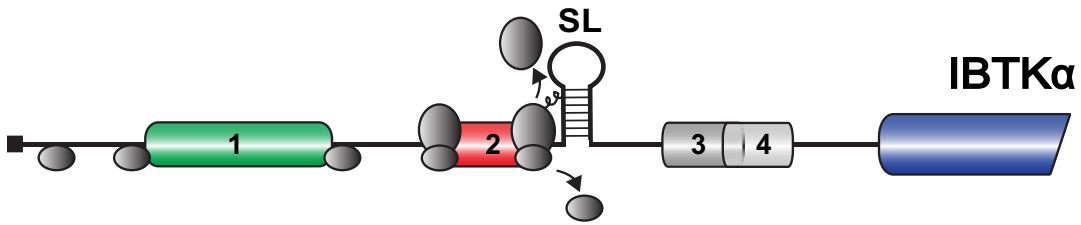
control can include uORFs and RNA secondary structures, which can function in combination to modulate translation efficiencies during the ISR.

Given the key results of this thesis, the following model was proposed for preferential translation *IBTK α* mRNA during the ISR (Figure 18). In the absence of stress, there is low p-eIF2 α and abundant eIF2-GTP to deliver initiator tRNA to the translational machinery. In this condition, the preinitiation ribosome complex containing 40S ribosomal subunits is thought to bind to the 5'-end cap structure, processively scan and predominantly translate uORF2. In the illustrated model, the 40S ribosomal subunit recognizes the start codon of uORF2 (red box) and subsequently joins with the 60S subunit to proceed with translation elongation of the short uORF2 coding sequence. The uORF2 is a major inhibitor of *IBTK α* CDS translation and functions in conjunction with the downstream SL to sharply reduce translation reinitiation at downstream coding sequences. Therefore, following translation of uORF2, ribosomes dissociate from the mRNA and there is reduced translation at the downstream *IBTK α* CDS. Upon stress and enhanced p-eIF2 α levels, there is lowered eIF2 ternary complex. It is suggested that some ribosomes can translate the 5'-proximal uORF1 (green box), allowing for efficient reinitiation at downstream coding sequences. Due to its proximity, translation of uORF1 is suggested to preclude translation of uORF2. Once the retained scanning ribosomes proceed through the inhibitory uORF2, there is reacquisition of the eIF2/GTP/Met-tRNA^{Met} complex that facilitates recognition of the start codon of the *IBTK α* CDS and enhanced synthesis of the *IBTK α* polypeptide. It is important to note that there is minimal translation of uORF3 and uORF4 (indicated as gray boxes) and their removal does not affect preferential translation of human *IBTK α* . Furthermore, while uORF3 and

uORF4 are present in humans and rodents they are absent in other mammals, supporting the idea that these elements are dispensable for *IBTK α* translational control. An additional mechanism enhancing *IBTK α* translation may involve p-eIF2 α -induced ribosome bypass or leaky scanning through the uORFs and direct ribosome initiation at the *IBTK α* CDS. In this illustration, scanning and elongating ribosomes are illustrated by the ovals.

Blocking re-initiation and Ribosome bypass

No Stress: High eIF2-GTP, low eIF2 α -P



High Stress: Low eIF2-GTP, high eIF2 α -P

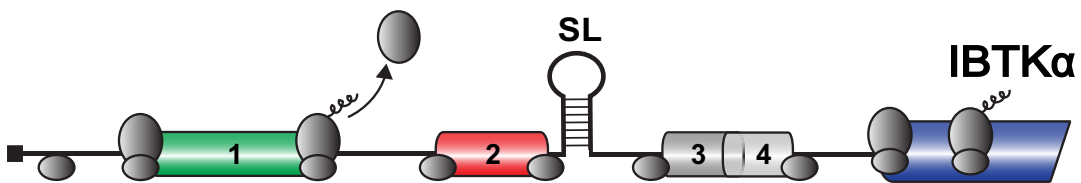


Figure 18. Model of preferential translation of human *IBTKα*.

The uORFs in the *IBTKα* mRNA are represented as boxes situated upstream of the CDS encoding the IBTK α protein. A model of translation control of *IBTKα* mRNA during stress in the ISR is described in the text.

4.2 RNA elements that confer preferential translation in the ISR

Various cis-acting elements are present on the 5'-leader sequence of an mRNA that can affect translation. A majority of genome wide studies are focused on *in silico* prediction of canonical uORFs. There are several properties of translated uORFs that may enhance or deter translation reinitiation. An important goal is to use informatic tools to predict translation efficiencies of mRNAs in the ISR based on their 5'-leader sequences. In general, short uORFs are thought to retain critical initiation factors, such as eIF3, which enhance translation reinitiation (11,104,105). Alternatively, as reported for the ISR regulator *CHOP*, short uORFs can also encode specific codons that are thought to trigger elongation pauses that lead to poor ribosome reinitiation (50,51) (Figure 19). In the example of *GADD34*, the primary translated uORF2 encodes proline rich sequence just prior to the stop codon. This sequence is thought to alter termination processes, hindering translation reinitiation at the downstream CDS (67). Furthermore, *ATF4* and the related *ATF5* mRNAs have an inhibitory uORF2 that overlaps out-of-frame with the CDS, which would preclude ribosome recognition of the CDS start codons (52,53) (Figure 19). This study adds an additional mechanism whereby an RNA stem-loop structure just downstream of an uORF can work together to impede reinitiation (Figure 19). The folding stability of the SL in the *IBTK α* mRNA is $\Delta G^\circ = -20$ kcal/mol, which did not preclude ribosome scanning by itself. Depending on the placement, insertion of more stable stem-loop structures can function as a strong barrier to ribosome scanning (19). Therefore, along with the position downstream of uORF2 in the 5'-leader of the *IBTK α* mRNA, folding stability is suggested to be optimized to allow for the SL to work in synergy with the translated uORF2 to serve as a negative-element in the *IBTK α*

translational control. As a consequence, the model for *IBTK α* translational control presented here suggests that future mechanistic studies of the translational changes in the ISR genome-wide should integrate not only translated uORFs but also the proximity and stability of RNA secondary structures.

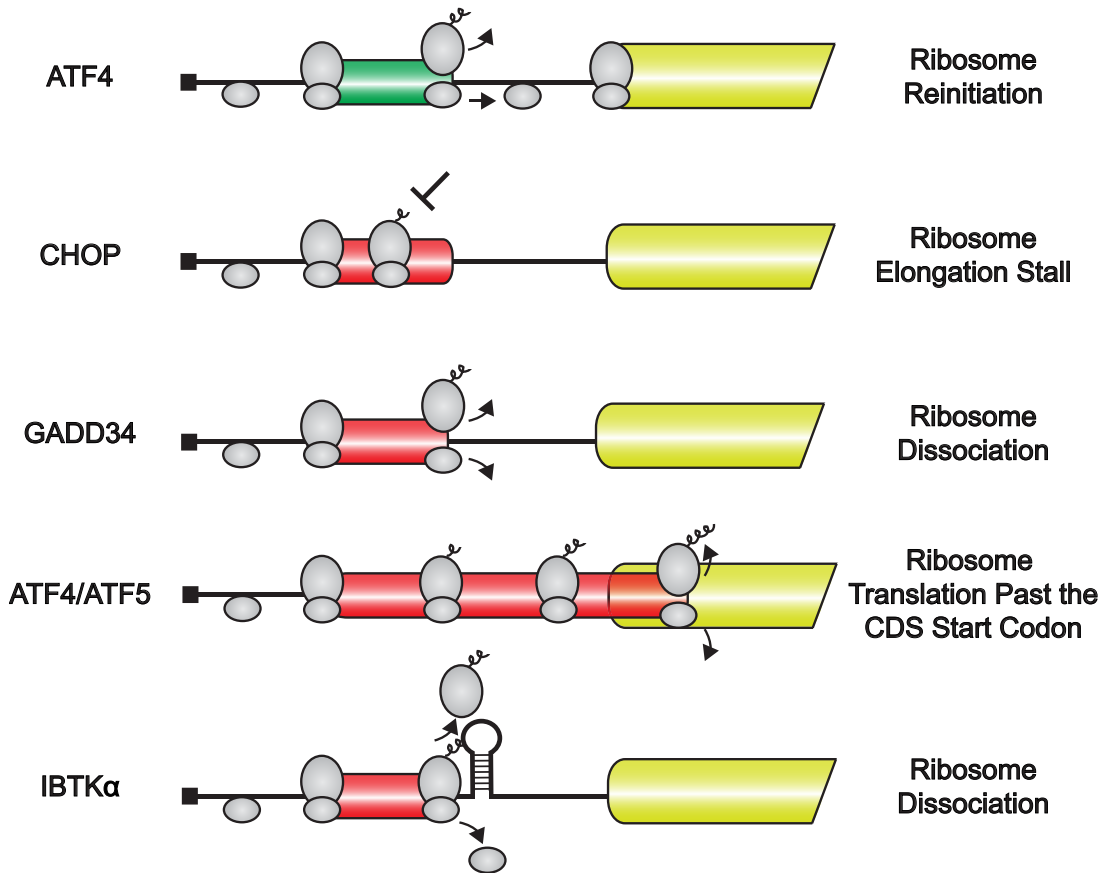


Figure 19. Different functions of uORFs in the ISR.

uORFs in the ISR can perform different functions, including promoting ribosome reinitiation after uORF translation (e.g. uORF1 in *ATF4* (53), ribosome elongation stalling during translation of an uORF as described for *CHOP* (50,51), altered translation termination and enhanced ribosome dissociation from the mRNA as reported for *GADD34* (67). Additionally, as described for the *ATF4* and *ATF5* uORF2, uORFs can be situated out-of-frame with the CDS and therefore uORF translation precludes that of the CDS (52,53). This study shows that the *IBTKα* uORF2 combines with a downstream SL to sharply lower ribosome reinitiation at downstream coding sequences. In this illustration, the CDS is indicated by the yellow bar. Positive-acting uORFs are indicated

by a green bar, whereas negative-acting uORFs are denoted as red bars. Scanning and elongating ribosomes are illustrated by the gray ovals. This illustration was adapted from a figure presented in a review by Young and Wek (10).

4.3 RNA structurome in the ISR

The cis-regulatory elements on the 5'-leader of an mRNA can regulate the process of translational control imposed in the ISR. One of the widely studied 5'-leader elements in translational regulation is the uORFs. Computational methods have allowed for identification of canonical uORFs genome-wide, and these efforts have been supplemented with experimental approaches, such as ribosome profiling, that serve to delineate which uORFs are translated through ribosome occupancy (106,107). It is noteworthy that these experimental approaches, including global translation initiation sequencing (GTI-Seq) and quantitative translation initiation sequencing (QTI-seq), have identified translation of uORFs with non-canonical start codons (61,62). It is also noted that experimental measurements of ribosome occupancy largely used standard cell lines and given the range of transcript expression and splicing variation between cell type among tissues, there is likely to be substantially more translated uORFs than reported. Together, these results suggest that the prevalence of translated uORFs may be much higher than predicted.

This study focused on *IBTK α* demonstrated that along with uORFs the secondary RNA structure present in the 5'-leader of an mRNA can significantly contribute to the translation regulation of a gene. This study also showcases the phylogenetic conservation of regulatory elements of *IBTK α* among mammals. An important goal is to utilize informatics approaches that will integrate the experimentally identified uORFs, phylogenetic conservation, and RNA structural elements flanking uORFs to predict translation efficiencies of mRNAs in ISR and their underlying mechanisms. The recent advent in methods such as dimethyl sulfate (DMS)-mutational profiling with sequencing

(DMS-MaPseq) which allows in vivo RNA structure prediction can be used to determine RNA structure of 5'-leaders of mRNAs in cells treated with ISR inducers (108,109). It is suggested that many gene transcript possess secondary RNA stem-loops with significant stability in their 5'-leaders, but a genome wide experimental analysis of these structures has not yet been well documented. This thesis suggests that secondary RNA structures with moderate stability, such as that described for *IBTK α* , can be present in the 5'-leaders of other mRNAs and can regulate their translation. For example, the 5'-leader of *TGF- β_1* was reported to possess a conserved secondary RNA stem-loop with moderate stability that lowers the translation efficiency of *TGF- β_1* mRNA. The study suggested that regulatory factors like DDX3 remodels 5'-leader of *TGF- β_1* to overcome inhibitory effect of the stem-loop and induce TGF- β_1 synthesis (110,111). The approach of integrating the RNA structure information in combination with uORFs will provide a better understanding of the extent to which uORFs in combination with SLs contribute to translation control during the ISR.

4.4 Significance of this study

This study provides a better understanding of the mechanism by which expression of *IBTK α* is regulated in the basal as well as during ER stress conditions. Short uORFs usually are suggested to promote translation reinitiation from the downstream initiation site. However, this translational control study of *IBTK α* demonstrated that the short uORF can block reinitiation by utilizing the flanking RNA structural elements. Therefore, predictive tools for assessing uORF functions in translational control should account for the presence of SL structures flanking the stop codons. In the future, it will be important

to identify other cellular mRNAs that possess a similar arrangement of shorter uORF and a flanking stem-loop element in their 5'-leader like *IBTK α* to determine the mode of translational regulation presented is unique to *IBTK α* or is common among other cellular mRNAs.

4.5 Implications of IBTK α in the ISR implementation and function

A prior study has shown that the transcription induction of *IBTK α* is dependent on ATF4 during ER stress (28). It was suggested that there is a significant reduction in *IBTK α* protein levels in mice with a liver specific PERK knock-out that were subjected to pharmacological induction of ER stress (28). Based on the prior reports as well as the immunoblot results of *IBTK α* from the time course experiment with Tg depicted in this thesis (Figure 8), induction of *IBTK α* expression occurs late during ER stress. The misfolded or unfolded protein aggregates are formed in the ER lumen in the late phase of ER stress. Two pathways- endoplasmic reticulum associated degradation (ERAD) and autophagy play an essential role in degradation of these problematic proteins, serving to help restore the function and processing capacity of ER (60). *IBTK α* is suggested to facilitate ubiquitination of target proteins by functioning as an adapter for E3 ubiquitin ligase. *IBTK α* is suggested to interact with CUL3 on its C-terminal end through BTB domains and the other target proteins on its N-terminal end through RCC1 domain and ankyrin repeats and thereby mediates the transfer of ubiquitin from CUL3 to the proteins targeted for degradation. The strategic location of *IBTK α* on ER membrane and ER exit sites suggests that *IBTK α* may play an important role in ERAD. An important future question is to study the function of *IBTK α* in ERAD. The timing of expression of ISR

effectors is very critical as each is required at different stages of ISR. The ISR fine tunes the gene expression program by transcriptional and translation induction of ISR regulators to ensure the expression of ISR effectors in a timely manner. Therefore, the later induction of IBTK α may be central for proposed protein clearance that occurs with stress.

REFERENCES

1. Ingolia, N. T. (2014) Ribosome profiling: new views of translation, from single codons to genome scale. *Nat Rev Genet* **15**, 205-213
2. Hinnebusch, A. G. (2014) The scanning mechanism of eukaryotic translation initiation. *Annu Rev Biochem* **83**, 779-812
3. Hinnebusch, A. G., and Lorsch, J. R. (2012) The mechanism of eukaryotic translation initiation: new insights and challenges. *Cold Spring Harb Perspect Biol* **4**
4. Sonenberg, N., and Hinnebusch, A. G. (2009) Regulation of translation initiation in eukaryotes: mechanisms and biological targets. *Cell* **136**, 731-745
5. Dever, T. E., Dinman, J. D., and Green, R. (2018) Translation elongation and recoding in eukaryotes. *Cold Spring Harb Perspect Biol* **10**
6. Dever, T. E., and Green, R. (2012) The elongation, termination, and recycling phases of translation in eukaryotes. *Cold Spring Harb Perspect Biol* **4**, a013706
7. Hellen, C. U. T. (2018) Translation termination and ribosome recycling in eukaryotes. *Cold Spring Harb Perspect Biol* **10**
8. Alkalaeva, E. Z., Pisarev, A. V., Frolova, L. Y., Kisselev, L. L., and Pestova, T. V. (2006) In vitro reconstitution of eukaryotic translation reveals cooperativity between release factors eRF1 and eRF3. *Cell* **125**, 1125-1136
9. Wek, R. C. (2018) Role of eIF2alpha kinases in translational control and adaptation to cellular stress. *Cold Spring Harb Perspect Biol* **10**

10. Young, S. K., and Wek, R. C. (2016) Upstream open reading frames differentially regulate gene-specific translation in the integrated stress response. *J Biol Chem* **291**, 16927-16935
11. Hinnebusch, A. G., Ivanov, I. P., and Sonenberg, N. (2016) Translational control by 5'-untranslated regions of eukaryotic mRNAs. *Science* **352**, 1413-1416
12. Lejbkowitz, F., Goyer, C., Darveau, A., Neron, S., Lemieux, R., and Sonenberg, N. (1992) A fraction of the mRNA 5' cap-binding protein, eukaryotic initiation factor 4E, localizes to the nucleus. *Proc Natl Acad Sci U S A* **89**, 9612-9616
13. Wells, S. E., Hillner, P. E., Vale, R. D., and Sachs, A. B. (1998) Circularization of mRNA by eukaryotic translation initiation factors. *Mol Cell* **2**, 135-140
14. Derry, M. C., Yanagiya, A., Martineau, Y., and Sonenberg, N. (2006) Regulation of poly(A)-binding protein through PABP-interacting proteins. *Cold Spring Harb Symp Quant Biol* **71**, 537-543
15. Liu, B., and Qian, S. B. (2014) Translational reprogramming in cellular stress response. *Wiley Interdiscip Rev RNA* **5**, 301-315
16. Calvo, S. E., Pagliarini, D. J., and Mootha, V. K. (2009) Upstream open reading frames cause widespread reduction of protein expression and are polymorphic among humans. *Proc Natl Acad Sci U S A* **106**, 7507-7512
17. Iacono, M., Mignone, F., and Pesole, G. (2005) uAUG and uORFs in human and rodent 5'untranslated mRNAs. *Gene* **349**, 97-105
18. Resch, A. M., Ogurtsov, A. Y., Rogozin, I. B., Shabalina, S. A., and Koonin, E. V. (2009) Evolution of alternative and constitutive regions of mammalian 5'UTRs. *BMC Genomics* **10**, 162

19. Kozak, M. (1989) Circumstances and mechanisms of inhibition of translation by secondary structure in eucaryotic mRNAs. *Mol Cell Biol* **9**, 5134-5142
20. Chase, A. J., and Semler, B. L. (2012) Viral subversion of host functions for picornavirus translation and RNA replication. *Future Virol* **7**, 179-191
21. Fernandez, J., Yaman, I., Huang, C., Liu, H., Lopez, A. B., Komar, A. A., Caprara, M. G., Merrick, W. C., Snider, M. D., Kaufman, R. J., Lamers, W. H., and Hatzoglou, M. (2005) Ribosome stalling regulates IRES-mediated translation in eukaryotes, a parallel to prokaryotic attenuation. *Mol Cell* **17**, 405-416
22. Yaman, I., Fernandez, J., Liu, H., Caprara, M., Komar, A. A., Koromilas, A. E., Zhou, L., Snider, M. D., Scheuner, D., Kaufman, R. J., and Hatzoglou, M. (2003) The zipper model of translational control: a small upstream ORF is the switch that controls structural remodeling of an mRNA leader. *Cell* **113**, 519-531
23. Muckenthaler, M., Gray, N. K., and Hentze, M. W. (1998) IRP-1 binding to ferritin mRNA prevents the recruitment of the small ribosomal subunit by the cap-binding complex eIF4F. *Mol Cell* **2**, 383-388
24. Gray, N. K., and Hentze, M. W. (1994) Iron regulatory protein prevents binding of the 43S translation pre-initiation complex to ferritin and eALAS mRNAs. *EMBO J* **13**, 3882-3891
25. Liu, Y., Yang, Q., and Zhao, F. (2021) Synonymous but not silent: the codon usage code for gene expression and protein folding. *Annu Rev Biochem* **90**, 375-401

26. O'Brien, J., Hayder, H., Zayed, Y., and Peng, C. (2018) Overview of microRNA biogenesis, mechanisms of actions, and circulation. *Front Endocrinol (Lausanne)* **9**, 402
27. Essig, K., Kronbeck, N., Guimaraes, J. C., Lohs, C., Schlundt, A., Hoffmann, A., Behrens, G., Brenner, S., Kowalska, J., Lopez-Rodriguez, C., Jemielity, J., Holtmann, H., Reiche, K., Hackermuller, J., Sattler, M., Zavolan, M., and Heissmeyer, V. (2018) Roquin targets mRNAs in a 3'-UTR-specific manner by different modes of regulation. *Nat Commun* **9**, 3810
28. Baird, T. D., Palam, L. R., Fusakio, M. E., Willy, J. A., Davis, C. M., McClintick, J. N., Anthony, T. G., and Wek, R. C. (2014) Selective mRNA translation during eIF2 phosphorylation induces expression of IBTKalpha. *Mol Biol Cell* **25**, 1686-1697
29. Zyryanova, A. F., Kashiwagi, K., Rato, C., Harding, H. P., Crespillo-Casado, A., Perera, L. A., Sakamoto, A., Nishimoto, M., Yonemochi, M., Shirouzu, M., Ito, T., and Ron, D. (2021) ISRIB blunts the integrated stress response by allosterically antagonising the inhibitory effect of phosphorylated eIF2 on eIF2B. *Mol Cell* **81**, 88-103 e106
30. Schoof, M., Boone, M., Wang, L., Lawrence, R., Frost, A., and Walter, P. (2021) eIF2B conformation and assembly state regulate the integrated stress response. *Elife* **10**
31. Jousse, C., Oyadomari, S., Novoa, I., Lu, P., Zhang, Y., Harding, H. P., and Ron, D. (2003) Inhibition of a constitutive translation initiation factor 2alpha phosphatase, CReP, promotes survival of stressed cells. *J Cell Biol* **163**, 767-775

32. Novoa, I., Zeng, H., Harding, H. P., and Ron, D. (2001) Feedback inhibition of the unfolded protein response by GADD34-mediated dephosphorylation of eIF2alpha. *J Cell Biol* **153**, 1011-1022
33. Ma, Y., and Hendershot, L. M. (2003) Delineation of a negative feedback regulatory loop that controls protein translation during endoplasmic reticulum stress. *J Biol Chem* **278**, 34864-34873
34. Connor, J. H., Weiser, D. C., Li, S., Hallenbeck, J. M., and Shenolikar, S. (2001) Growth arrest and DNA damage-inducible protein GADD34 assembles a novel signaling complex containing protein phosphatase 1 and inhibitor 1. *Mol Cell Biol* **21**, 6841-6850
35. Costa-Mattioli, M., and Walter, P. (2020) The integrated stress response: from mechanism to disease. *Science* **368**
36. Chen, J. J. (2014) Translational control by heme-regulated eIF2alpha kinase during erythropoiesis. *Curr Opin Hematol* **21**, 172-178
37. Guo, X., Aviles, G., Liu, Y., Tian, R., Unger, B. A., Lin, Y. T., Wiita, A. P., Xu, K., Correia, M. A., and Kampmann, M. (2020) Mitochondrial stress is relayed to the cytosol by an OMA1-DELE1-HRI pathway. *Nature* **579**, 427-432
38. Dey, M., Cao, C., Dar, A. C., Tamura, T., Ozato, K., Sicheri, F., and Dever, T. E. (2005) Mechanistic link between PKR dimerization, autophosphorylation, and eIF2alpha substrate recognition. *Cell* **122**, 901-913
39. Garcia, M. A., Meurs, E. F., and Esteban, M. (2007) The dsRNA protein kinase PKR: virus and cell control. *Biochimie* **89**, 799-811

40. Shi, Y., Vattem, K. M., Sood, R., An, J., Liang, J., Stramm, L., and Wek, R. C. (1998) Identification and characterization of pancreatic eukaryotic initiation factor 2 alpha-subunit kinase, PEK, involved in translational control. *Mol Cell Biol* **18**, 7499-7509
41. Wang, P., Li, J., Tao, J., and Sha, B. (2018) The luminal domain of the ER stress sensor protein PERK binds misfolded proteins and thereby triggers PERK oligomerization. *J Biol Chem* **293**, 4110-4121
42. Koumenis, C., Naczki, C., Koritzinsky, M., Rastani, S., Diehl, A., Sonenberg, N., Koromilas, A., and Wouters, B. G. (2002) Regulation of protein synthesis by hypoxia via activation of the endoplasmic reticulum kinase PERK and phosphorylation of the translation initiation factor eIF2alpha. *Mol Cell Biol* **22**, 7405-7416
43. Dong, J., Qiu, H., Garcia-Barrio, M., Anderson, J., and Hinnebusch, A. G. (2000) Uncharged tRNA activates GCN2 by displacing the protein kinase moiety from a bipartite tRNA-binding domain. *Mol Cell* **6**, 269-279
44. Baird, T. D., and Wek, R. C. (2012) Eukaryotic initiation factor 2 phosphorylation and translational control in metabolism. *Adv Nutr* **3**, 307-321
45. Wu, C. C., Peterson, A., Zinshteyn, B., Regot, S., and Green, R. (2020) Ribosome collisions trigger general stress responses to regulate cell fate. *Cell* **182**, 404-416 e414
46. Deng, J., Harding, H. P., Raught, B., Gingras, A. C., Berlanga, J. J., Scheuner, D., Kaufman, R. J., Ron, D., and Sonenberg, N. (2002) Activation of GCN2 in UV-irradiated cells inhibits translation. *Curr Biol* **12**, 1279-1286

47. Collier, A. E., Wek, R. C., and Spandau, D. F. (2017) Human keratinocyte differentiation requires translational control by the eIF2alpha kinase GCN2. *J Invest Dermatol* **137**, 1924-1934
48. Scheu, S., Stetson, D. B., Reinhardt, R. L., Leber, J. H., Mohrs, M., and Locksley, R. M. (2006) Activation of the integrated stress response during T helper cell differentiation. *Nat Immunol* **7**, 644-651
49. Licari, E., Sanchez-Del-Campo, L., and Falletta, P. (2021) The two faces of the integrated stress response in cancer progression and therapeutic strategies. *Int J Biochem Cell Biol* **139**, 106059
50. Young, S. K., Palam, L. R., Wu, C., Sachs, M. S., and Wek, R. C. (2016) Ribosome elongation stall directs gene-specific translation in the integrated stress response. *J Biol Chem* **291**, 6546-6558
51. Palam, L. R., Baird, T. D., and Wek, R. C. (2011) Phosphorylation of eIF2 facilitates ribosomal bypass of an inhibitory upstream ORF to enhance CHOP translation. *J Biol Chem* **286**, 10939-10949
52. Zhou, D., Palam, L. R., Jiang, L., Narasimhan, J., Staschke, K. A., and Wek, R. C. (2008) Phosphorylation of eIF2 directs ATF5 translational control in response to diverse stress conditions. *J Biol Chem* **283**, 7064-7073
53. Vattam, K. M., and Wek, R. C. (2004) Reinitiation involving upstream ORFs regulates ATF4 mRNA translation in mammalian cells. *Proc Natl Acad Sci U S A* **101**, 11269-11274
54. Ameri, K., and Harris, A. L. (2008) Activating transcription factor 4. *Int J Biochem Cell Biol* **40**, 14-21

55. Fawcett, T. W., Martindale, J. L., Guyton, K. Z., Hai, T., and Holbrook, N. J. (1999) Complexes containing activating transcription factor (ATF)/cAMP-responsive-element-binding protein (CREB) interact with the CCAAT/enhancer-binding protein (C/EBP)-ATF composite site to regulate Gadd153 expression during the stress response. *Biochem J* **339** (Pt 1), 135-141
56. Harding, H. P., Zhang, Y., Zeng, H., Novoa, I., Lu, P. D., Calton, M., Sadri, N., Yun, C., Popko, B., Paules, R., Stojdl, D. F., Bell, J. C., Hettmann, T., Leiden, J. M., and Ron, D. (2003) An integrated stress response regulates amino acid metabolism and resistance to oxidative stress. *Mol Cell* **11**, 619-633
57. Harding, H. P., Novoa, I., Zhang, Y., Zeng, H., Wek, R., Schapira, M., and Ron, D. (2000) Regulated translation initiation controls stress-induced gene expression in mammalian cells. *Mol Cell* **6**, 1099-1108
58. Morita, M., Gravel, S. P., Chenard, V., Sikstrom, K., Zheng, L., Alain, T., Gandin, V., Avizonis, D., Arguello, M., Zakaria, C., McLaughlan, S., Nouet, Y., Pause, A., Pollak, M., Gottlieb, E., Larsson, O., St-Pierre, J., Topisirovic, I., and Sonenberg, N. (2013) mTORC1 controls mitochondrial activity and biogenesis through 4E-BP-dependent translational regulation. *Cell Metab* **18**, 698-711
59. Scheuner, D., Song, B., McEwen, E., Liu, C., Laybutt, R., Gillespie, P., Saunders, T., Bonner-Weir, S., and Kaufman, R. J. (2001) Translational control is required for the unfolded protein response and in vivo glucose homeostasis. *Mol Cell* **7**, 1165-1176

60. Bhattarai, K. R., Riaz, T. A., Kim, H. R., and Chae, H. J. (2021) The aftermath of the interplay between the endoplasmic reticulum stress response and redox signaling. *Exp Mol Med* **53**, 151-167
61. Lee, S., Liu, B., Lee, S., Huang, S. X., Shen, B., and Qian, S. B. (2012) Global mapping of translation initiation sites in mammalian cells at single-nucleotide resolution. *Proc Natl Acad Sci U S A* **109**, E2424-2432
62. Gao, X., Wan, J., Liu, B., Ma, M., Shen, B., and Qian, S. B. (2015) Quantitative profiling of initiating ribosomes in vivo. *Nat Methods* **12**, 147-153
63. Dever, T. E., Ivanov, I. P., and Sachs, M. S. (2020) Conserved upstream open reading frame nascent peptides that control translation. *Annu Rev Genet* **54**, 237-264
64. Kozak, M. (1989) The scanning model for translation: an update. *J Cell Biol* **108**, 229-241
65. Kozak, M. (1986) Point mutations define a sequence flanking the AUG initiator codon that modulates translation by eukaryotic ribosomes. *Cell* **44**, 283-292
66. Pisarev, A. V., Kolupaeva, V. G., Pisareva, V. P., Merrick, W. C., Hellen, C. U., and Pestova, T. V. (2006) Specific functional interactions of nucleotides at key -3 and +4 positions flanking the initiation codon with components of the mammalian 48S translation initiation complex. *Genes Dev* **20**, 624-636
67. Young, S. K., Willy, J. A., Wu, C., Sachs, M. S., and Wek, R. C. (2015) Ribosome reinitiation directs gene-specific translation and regulates the integrated stress response. *J Biol Chem* **290**, 28257-28271

68. Andreev, D. E., Arnold, M., Kiniry, S. J., Loughran, G., Michel, A. M., Rachinskii, D., and Baranov, P. V. (2018) TASEP modelling provides a parsimonious explanation for the ability of a single uORF to derepress translation during the integrated stress response. *Elife* **7**
69. Kozak, M. (1990) Downstream secondary structure facilitates recognition of initiator codons by eukaryotic ribosomes. *Proc Natl Acad Sci U S A* **87**, 8301-8305
70. Delepine, M., Nicolino, M., Barrett, T., Golamaully, M., Lathrop, G. M., and Julier, C. (2000) EIF2AK3, encoding translation initiation factor 2-alpha kinase 3, is mutated in patients with Wolcott-Rallison syndrome. *Nat Genet* **25**, 406-409
71. Eyries, M., Montani, D., Girerd, B., Perret, C., Leroy, A., Lonjou, C., Chelghoum, N., Coulet, F., Bonnet, D., Dorfmueller, P., Fadel, E., Sitbon, O., Simonneau, G., Tregouet, D. A., Humbert, M., and Soubrier, F. (2014) EIF2AK4 mutations cause pulmonary veno-occlusive disease, a recessive form of pulmonary hypertension. *Nat Genet* **46**, 65-69
72. Harding, H. P., Zeng, H., Zhang, Y., Jungries, R., Chung, P., Plesken, H., Sabatini, D. D., and Ron, D. (2001) Diabetes mellitus and exocrine pancreatic dysfunction in *perk*^{-/-} mice reveals a role for translational control in secretory cell survival. *Mol Cell* **7**, 1153-1163
73. Zhang, P., McGrath, B., Li, S., Frank, A., Zambito, F., Reinert, J., Gannon, M., Ma, K., McNaughton, K., and Cavener, D. R. (2002) The PERK eukaryotic initiation factor 2 alpha kinase is required for the development of the skeletal

- system, postnatal growth, and the function and viability of the pancreas. *Mol Cell Biol* **22**, 3864-3874
74. Abdulkarim, B., Nicolino, M., Igoillo-Esteve, M., Daures, M., Romero, S., Philippi, A., Senee, V., Lopes, M., Cunha, D. A., Harding, H. P., Derbois, C., Bendelac, N., Hattersley, A. T., Eizirik, D. L., Ron, D., Cnop, M., and Julier, C. (2015) A missense mutation in PPP1R15B causes a syndrome including diabetes, short stature, and microcephaly. *Diabetes* **64**, 3951-3962
75. Kernohan, K. D., Tetreault, M., Liwak-Muir, U., Geraghty, M. T., Qin, W., Venkateswaran, S., Davila, J., Care4Rare Canada, C., Holcik, M., Majewski, J., Richer, J., and Boycott, K. M. (2015) Homozygous mutation in the eukaryotic translation initiation factor 2alpha phosphatase gene, PPP1R15B, is associated with severe microcephaly, short stature and intellectual disability. *Hum Mol Genet* **24**, 6293-6300
76. van der Knaap, M. S., Leegwater, P. A., Konst, A. A., Visser, A., Naidu, S., Oudejans, C. B., Schutgens, R. B., and Pronk, J. C. (2002) Mutations in each of the five subunits of translation initiation factor eIF2B can cause leukoencephalopathy with vanishing white matter. *Ann Neurol* **51**, 264-270
77. Leegwater, P. A., Vermeulen, G., Konst, A. A., Naidu, S., Mulders, J., Visser, A., Kersbergen, P., Mobach, D., Fonds, D., van Berkel, C. G., Lemmers, R. J., Frants, R. R., Oudejans, C. B., Schutgens, R. B., Pronk, J. C., and van der Knaap, M. S. (2001) Subunits of the translation initiation factor eIF2B are mutant in leukoencephalopathy with vanishing white matter. *Nat Genet* **29**, 383-388

78. Skopkova, M., Hennig, F., Shin, B. S., Turner, C. E., Stanikova, D., Brennerova, K., Stanik, J., Fischer, U., Henden, L., Muller, U., Steinberger, D., Leshinsky-Silver, E., Bottani, A., Kurdiova, T., Ukropec, J., Nyitrayova, O., Kolnikova, M., Klimes, I., Borck, G., Bahlo, M., Haas, S. A., Kim, J. R., Lotspeich-Cole, L. E., Gasperikova, D., Dever, T. E., and Kalscheuer, V. M. (2017) EIF2S3 mutations associated with severe X-linked intellectual disability syndrome MEHMO. *Hum Mutat* **38**, 409-425
79. Gregory, L. C., Ferreira, C. B., Young-Baird, S. K., Williams, H. J., Harakalova, M., van Haaften, G., Rahman, S. A., Gaston-Massuet, C., Kelberman, D., Gosgene, Qasim, W., Camper, S. A., Dever, T. E., Shah, P., Robinson, I., and Dattani, M. T. (2019) Impaired EIF2S3 function associated with a novel phenotype of X-linked hypopituitarism with glucose dysregulation. *EBioMedicine* **42**, 470-480
80. Moortgat, S., Desir, J., Benoit, V., Boulanger, S., Pendeville, H., Nassogne, M. C., Lederer, D., and Maystadt, I. (2016) Two novel EIF2S3 mutations associated with syndromic intellectual disability with severe microcephaly, growth retardation, and epilepsy. *Am J Med Genet A* **170**, 2927-2933
81. Nguyen, H. G., Conn, C. S., Kye, Y., Xue, L., Forester, C. M., Cowan, J. E., Hsieh, A. C., Cunningham, J. T., Truillet, C., Tameire, F., Evans, M. J., Evans, C. P., Yang, J. C., Hann, B., Koumenis, C., Walter, P., Carroll, P. R., and Ruggero, D. (2018) Development of a stress response therapy targeting aggressive prostate cancer. *Sci Transl Med* **10**

82. Abbink, T. E. M., Wisse, L. E., Jaku, E., Thiecke, M. J., Voltolini-Gonzalez, D., Fritsen, H., Bobeldijk, S., Ter Braak, T. J., Polder, E., Postma, N. L., Bugiani, M., Struijs, E. A., Verheijen, M., Straat, N., van der Sluis, S., Thomas, A. A. M., Molenaar, D., and van der Knaap, M. S. (2019) Vanishing white matter: deregulated integrated stress response as therapy target. *Ann Clin Transl Neurol* **6**, 1407-1422
83. Young-Baird, S. K., Lourenco, M. B., Elder, M. K., Klann, E., Liebau, S., and Dever, T. E. (2020) Suppression of MEHMO syndrome mutation in eIF2 by small molecule ISRIB. *Mol Cell* **77**, 875-886 e877
84. Atkins, C., Liu, Q., Minthorn, E., Zhang, S. Y., Figueroa, D. J., Moss, K., Stanley, T. B., Sanders, B., Goetz, A., Gaul, N., Choudhry, A. E., Alsaïd, H., Jucker, B. M., Axten, J. M., and Kumar, R. (2013) Characterization of a novel PERK kinase inhibitor with antitumor and antiangiogenic activity. *Cancer Res* **73**, 1993-2002
85. Fujimoto, J., Kurasawa, O., Takagi, T., Liu, X., Banno, H., Kojima, T., Asano, Y., Nakamura, A., Nambu, T., Hata, A., Ishii, T., Sameshima, T., Debori, Y., Miyamoto, M., Klein, M. G., Tjhen, R., Sang, B. C., Levin, I., Lane, S. W., Snell, G. P., Li, K., Kefala, G., Hoffman, I. D., Ding, S. C., Cary, D. R., and Mizojiri, R. (2019) Identification of novel, potent, and orally available GCN2 inhibitors with type I half binding mode. *ACS Med Chem Lett* **10**, 1498-1503
86. Das, I., Krzyzosiak, A., Schneider, K., Wrabetz, L., D'Antonio, M., Barry, N., Sigurdardottir, A., and Bertolotti, A. (2015) Preventing proteostasis diseases by selective inhibition of a phosphatase regulatory subunit. *Science* **348**, 239-242

87. Wang, L., Popko, B., Tixier, E., and Roos, R. P. (2014) Guanabenz, which enhances the unfolded protein response, ameliorates mutant SOD1-induced amyotrophic lateral sclerosis. *Neurobiol Dis* **71**, 317-324
88. Way, S. W., Podojil, J. R., Clayton, B. L., Zaremba, A., Collins, T. L., Kunjamma, R. B., Robinson, A. P., Brugarolas, P., Miller, R. H., Miller, S. D., and Popko, B. (2015) Pharmaceutical integrated stress response enhancement protects oligodendrocytes and provides a potential multiple sclerosis therapeutic. *Nat Commun* **6**, 6532
89. Chen, Y., Kunjamma, R. B., Weiner, M., Chan, J. R., and Popko, B. (2021) Prolonging the integrated stress response enhances CNS remyelination in an inflammatory environment. *Elife* **10**
90. Spatuzza, C., Schiavone, M., Di Salle, E., Janda, E., Sardiello, M., Fiume, G., Fierro, O., Simonetta, M., Argiriou, N., Faraonio, R., Capparelli, R., Quinto, I., and Scala, G. (2008) Physical and functional characterization of the genetic locus of IBtk, an inhibitor of Bruton's tyrosine kinase: evidence for three protein isoforms of IBtk. *Nucleic Acids Res* **36**, 4402-4416
91. Xu, L., Wei, Y., Reboul, J., Vaglio, P., Shin, T. H., Vidal, M., Elledge, S. J., and Harper, J. W. (2003) BTB proteins are substrate-specific adaptors in an SCF-like modular ubiquitin ligase containing CUL-3. *Nature* **425**, 316-321
92. Furukawa, M., He, Y. J., Borchers, C., and Xiong, Y. (2003) Targeting of protein ubiquitination by BTB-Cullin 3-Roc1 ubiquitin ligases. *Nat Cell Biol* **5**, 1001-1007

93. Willy, J. A., Young, S. K., Mosley, A. L., Gawrieh, S., Stevens, J. L., Masuoka, H. C., and Wek, R. C. (2017) Function of inhibitor of Bruton's tyrosine kinase isoform alpha (IBTKalpha) in nonalcoholic steatohepatitis links autophagy and the unfolded protein response. *J Biol Chem* **292**, 14050-14065
94. Pisano, A., Ceglia, S., Palmieri, C., Vecchio, E., Fiume, G., de Laurentiis, A., Mimmi, S., Falcone, C., Iaccino, E., Scialdone, A., Pontoriero, M., Masci, F. F., Valea, R., Krishnan, S., Gaspari, M., Cuda, G., Scala, G., and Quinto, I. (2015) CRL3IBTK regulates the tumor suppressor Pcd4 through ubiquitylation coupled to proteasomal degradation. *J Biol Chem* **290**, 13958-13971
95. Jin, L., Pahuja, K. B., Wickliffe, K. E., Gorur, A., Baumgartel, C., Schekman, R., and Rape, M. (2012) Ubiquitin-dependent regulation of COPII coat size and function. *Nature* **482**, 495-500
96. Blum, M., Chang, H. Y., Chuguransky, S., Grego, T., Kandasaamy, S., Mitchell, A., Nuka, G., Paysan-Lafosse, T., Qureshi, M., Raj, S., Richardson, L., Salazar, G. A., Williams, L., Bork, P., Bridge, A., Gough, J., Haft, D. H., Letunic, I., Marchler-Bauer, A., Mi, H., Natale, D. A., Necci, M., Orengo, C. A., Pandurangan, A. P., Rivoire, C., Sigrist, C. J. A., Sillitoe, I., Thanki, N., Thomas, P. D., Tosatto, S. C. E., Wu, C. H., Bateman, A., and Finn, R. D. (2021) The InterPro protein families and domains database: 20 years on. *Nucleic Acids Res* **49**, D344-D354
97. Jones, P., Binns, D., Chang, H. Y., Fraser, M., Li, W., McAnulla, C., McWilliam, H., Maslen, J., Mitchell, A., Nuka, G., Pesseat, S., Quinn, A. F., Sangrador-Vegas, A., Scheremetjew, M., Yong, S. Y., Lopez, R., and Hunter, S. (2014)

- InterProScan 5: genome-scale protein function classification. *Bioinformatics* **30**, 1236-1240
98. Conant, D., Hsiau, T., Rossi, N., Oki, J., Maures, T., Waite, K., Yang, J., Joshi, S., Kelso, R., Holden, K., Enzmann, B. L., and Stoner, R. (2022) Inference of CRISPR edits from sanger trace data. *CRISPR J* **5**, 123-130
99. Schneider, C. A., Rasband, W. S., and Eliceiri, K. W. (2012) NIH Image to ImageJ: 25 years of image analysis. *Nat Methods* **9**, 671-675
100. Teske, B. F., Baird, T. D., and Wek, R. C. (2011) Methods for analyzing eIF2 kinases and translational control in the unfolded protein response. *Methods Enzymol* **490**, 333-356
101. McWilliam, H., Li, W., Uludag, M., Squizzato, S., Park, Y. M., Buso, N., Cowley, A. P., and Lopez, R. (2013) Analysis tool web services from the EMBL-EBI. *Nucleic Acids Res* **41**, W597-600
102. Sievers, F., Wilm, A., Dineen, D., Gibson, T. J., Karplus, K., Li, W., Lopez, R., McWilliam, H., Remmert, M., Soding, J., Thompson, J. D., and Higgins, D. G. (2011) Fast, scalable generation of high-quality protein multiple sequence alignments using Clustal Omega. *Mol Syst Biol* **7**, 539
103. Gruber, A. R., Lorenz, R., Bernhart, S. H., Neubock, R., and Hofacker, I. L. (2008) The Vienna RNA websuite. *Nucleic Acids Res* **36**, W70-74
104. Mohammad, M. P., Munzarova Pondelickova, V., Zeman, J., Gunisova, S., and Valasek, L. S. (2017) In vivo evidence that eIF3 stays bound to ribosomes elongating and terminating on short upstream ORFs to promote reinitiation. *Nucleic Acids Res* **45**, 2658-2674

105. Szamecz, B., Rutkai, E., Cuchalova, L., Munzarova, V., Herrmannova, A., Nielsen, K. H., Burela, L., Hinnebusch, A. G., and Valasek, L. (2008) eIF3a cooperates with sequences 5' of uORF1 to promote resumption of scanning by post-termination ribosomes for reinitiation on GCN4 mRNA. *Genes Dev* **22**, 2414-2425
106. Ingolia, N. T., Ghaemmaghami, S., Newman, J. R., and Weissman, J. S. (2009) Genome-wide analysis in vivo of translation with nucleotide resolution using ribosome profiling. *Science* **324**, 218-223
107. Arribere, J. A., and Gilbert, W. V. (2013) Roles for transcript leaders in translation and mRNA decay revealed by transcript leader sequencing. *Genome Res* **23**, 977-987
108. Tomezsko, P., Swaminathan, H., and Rouskin, S. (2021) DMS-MaPseq for genome-wide or targeted RNA structure probing in vitro and in vivo. *Methods Mol Biol* **2254**, 219-238
109. Zubradt, M., Gupta, P., Persad, S., Lambowitz, A. M., Weissman, J. S., and Rouskin, S. (2017) DMS-MaPseq for genome-wide or targeted RNA structure probing in vivo. *Nat Methods* **14**, 75-82
110. Jenkins, R. H., Bennagi, R., Martin, J., Phillips, A. O., Redman, J. E., and Fraser, D. J. (2010) A conserved stem loop motif in the 5'untranslated region regulates transforming growth factor-beta(1) translation. *PLoS One* **5**, e12283
111. Lai, M. C., Lee, Y. H., and Tarn, W. Y. (2008) The DEAD-box RNA helicase DDX3 associates with export messenger ribonucleoproteins as well as tip-

associated protein and participates in translational control. *Mol Biol Cell* **19**,
3847-3858

CURRICULUM VITAE

Parth Hitenbhai Amin

Education

- Ph.D. in Biochemistry and Molecular Biology with minor in Bioinformatics
Indiana University earned at IUPUI, September 2022
- M.S. in Human Genetics
Virginia Commonwealth University, August 2016
- M.Sc. in Medical Biotechnology
Sardar Patel University, December 2013

Research Experience

- 2016-2022 Graduate Fellow, Mentor-Dr. Ronald C. Wek, IU School of
Medicine, Indianapolis, IN, USA
- Jan 2018- Aug 2018 Part Time Intern, Manager- Dr. Jeffrey A. Willy, Eli Lilly,
Indianapolis, IN, USA
- 2014-2016 Research Assistant, Mentor- Dr. Andrei Ivanov, VCU School of
Medicine, Richmond, VA, USA
- 2012 Research Assistant, Rajiv Gandhi Centre for Biotechnology,
Kerala, India
- 2008 Research Technician, Shree S.K Patel College of Pharmaceutical
Education and Research, Gujarat, India

Poster Presentations

- Experimental Biology meeting- April 2021
Presented poster titled “Inhibitor of Bruton’s Tyrosine Kinase- α in the Unfolded Protein Response” Parth H. Amin, Emily T. Mirek, Kirk A. Staschke, Tracy G. Anthony, Ronald C. Wek
- Cold Spring Harbor-Translational Control Meeting- September 2020
Presented poster titled “Regulation and function of IBTK α in the Unfolded Protein Response” Parth H. Amin, Kirk A. Staschke, Ronald C. Wek
- Gordon Research Conference-Contemporary Advances and Challenges in Drug Safety Assessment- June 2018
Presented poster titled “Transcription factors CHOP and NF- κ B regulate gene networks in non-alcoholic steatohepatitis” Parth H. Amin, Jiabin Qiu, Jeffrey A. Willy, Ronald C. Wek

Awards and Activities

- Graduate Student award from the Gordon Research Conference (2018) which covered the conference registration fees and travel
- Second Runner-up in Eureka Business Idea at SCIENTIFIQ organized by Charotar Vidhya Mandal, VV Nagar, India.
- Second Runner-up in Inter College Physics Quiz organized by Indian Physics Association
- Organized a Halloween themed science event on Halloween 2018 at Riley’s Children hospital, Indianapolis, IN

- Volunteered at Anatomy booth at Celebrate Science Indiana (2018), Indianapolis, IN

Publications

- **Amin, P. H.**, Carlson, K. R., Wek, R. C. (2022). An RNA stem-loop functions in conjunction with an upstream open reading frame to direct preferential translation in the integrated stress response. *Under review*
- Cordova, R., Misra, J., **Amin, P. H.**, Klunk, A. K., Damayanti, N. P., Carlson, K. R., Elmendorf, A., Kim, H. G., Mirek, E. T., Miller M., Dong, X. C., Anthony, T. G., Pili, R., Wek, R. C., Staschke, K. A. (2022). GCN2 eIF2 kinase promotes prostate cancer by maintaining amino acid homeostasis. *Under review*
- Miles, R. R., **Amin, P. H.**, Diaz, M. B., Misra, J., Aukerman, E., Das, A., Ghosh, N., Guith, T., Knierman, M. D., Roy, S., Spandau, D. F., & Wek, R. C. (2021). The eIF2 kinase GCN2 directs keratinocyte collective cell migration during wound healing via coordination of reactive oxygen species and amino acids. *The Journal of biological chemistry*, 101257.
- Augusto, L., Martynowicz, J., **Amin, P. H.**, Carlson, K. R., Wek, R. C., & Sullivan, W. J., Jr (2021). TgIF2K-B Is an eIF2 α Kinase in *Toxoplasma gondii* That Responds to Oxidative Stress and Optimizes Pathogenicity. *mBio*, 12(1), e03160-20.
- Augusto, L., Martynowicz, J., **Amin, P. H.**, Alakhras, N. S., Kaplan, M. H., Wek, R. C., & Sullivan, W. J., Jr (2020). *Toxoplasma gondii* Co-opts the Unfolded Protein Response To Enhance Migration and Dissemination of Infected Host Cells. *mBio*, 11(4), e00915-20.

- Augusto, L., **Amin, P. H.**, Wek, R. C., & Sullivan, W. J., Jr (2019). Regulation of arginine transport by GCN2 eIF2 kinase is important for replication of the intracellular parasite *Toxoplasma gondii*. *PLoS pathogens*, 15(6), e1007746.
- Lechuga, S., **Amin, P. H.**, Wolen, A. R., & Ivanov, A. I. (2019). Adducins inhibit lung cancer cell migration through mechanisms involving regulation of cell-matrix adhesion and cadherin-11 expression. *Biochimica et biophysica acta. Molecular cell research*, 1866(3), 395–408.
- Vinjamur, D. S., Alhashem, Y. N., Mohamad, S. F., **Amin, P.**, Williams, D. C., Jr, & Lloyd, J. A. (2016). Krüppel-Like Transcription Factor KLF1 Is Required for Optimal γ - and β -Globin Expression in Human Fetal Erythroblasts. *PloS one*, 11(2), e0146802.